

SIMULATION OF SOME ENGINEERING MEASURES AIMING AT  
REDUCING EFFECTS FROM EUTROPHICATION OF THE BALTIC SEA

Bo G. Gustafsson<sup>a,b</sup>, H. E. Markus Meier<sup>c,d</sup>, Oleg P. Savchuk<sup>b</sup>, Kari Eilola<sup>c</sup>, Lars Axell<sup>c</sup>,  
and Elin Almroth<sup>c</sup>

<sup>a</sup>*Oceanography – Earth Sciences Center, Göteborg University, Göteborg, Sweden*

<sup>b</sup>*Baltic Nest Institute, Stockholm University, Stockholm, Sweden*

<sup>c</sup>*Swedish Meteorological and Hydrological Institute, Norrköping, Sweden*

<sup>d</sup>*Department of Meteorology, Stockholm University, Stockholm, Sweden*



## Summary and conclusions

Two state of the art coupled physical-biogeochemical models have been used; RCO-SCOBİ developed at Swedish Meteorological and Hydrological Institute (SMHI) and BALTSEM developed at Göteborg University (GU) and Stockholm University (SU). The models are structurally different in that RCO-SCOBİ is a 3D model while BALTSEM resolves spatially the Baltic in 13 sub-basins. The biogeochemical sub-models have clear similarities, but there are significant differences as well. Both models reproduce present conditions with considerable accuracy.

The response on hydrography and eutrophication in the Baltic Sea to different engineering measures has been investigated with the models by simulations of a series of test cases:

- Case 0. Control case without any alterations
- Case 1. Halocline ventilation – the idea put forward by Stigebrandt and Gustafsson (2007) to pump water from 50 to 120 m depth
- Case 2. The salt lock – the idea by the O<sub>2</sub>-gruppen that is based on regulating flows through the Great Belt ([www.o2gruppen.se](http://www.o2gruppen.se))
- Case 3. Opening/closing of the straits – not really seriously proposed by anyone, but the discussion on the effects of general increasing/decreasing flow capacity of the straits is coming up regularly
  - Case 3a. Closed Öresund at the Drogden Sill
  - Case 3b. Dredged Drogden Sill to twice the present depth
- Case 4. Deep water oxygenation – supply oxygen to the deep water in sufficient amounts to keep the water from being hypoxic without disturbing stratification

From the simulations the following conclusions could be made:

- Feedbacks from *oxygen deficiency cause both increased primary production* in general and *increased cyanobacteria production* in particular. The theoretical supply of oxygen needed to curb oxygen deficiency is of the order of  $2 - 6 \times 10^6$  tons/yr.
- Any measures affecting the water exchange through the Danish Straits will cause salinity changes in the Baltic. The models show consistently that measures causing increased salinity also cause deteriorating oxygen conditions and those causing

decreased salinity improved oxygen conditions. However, freshening cases cause a long transitional stagnation period in deeper parts during which anoxia prevails. Thus, we conclude that *it is not possible to improve rapidly oxygen conditions by any realistic engineering method affecting the exchange through the Danish straits.*

- The models, in quite close agreement, show that halocline ventilation gives improved oxygen concentrations and no change in surface salinity. There is a decrease in deep-water salinity, but within the range of natural variability and should therefore not affect biodiversity. *Halocline ventilation is the only measure that cannot be ruled out* in this investigation.
- *The models give consistent and plausible responses.* However, we found quantitative differences in sensitivity and the reasons for these are explained.
- To accurately quantify the effects we need to improve in particular sediment parameterizations. Complementary high-resolution simulations are also necessary.

## **1 Introduction**

In recent years a number of engineering solutions has been proposed to improve oxygen conditions in deep waters of the Baltic proper. To investigate some of these suggestions we made simulations of the engineering solutions specified below with two models, BALTSEM and RCO-SCOBI. In this project, simulations have been done with the models without any modifications more than implementing the engineering solutions.

BALTSEM is a coupled physical-biogeochemical mechanistic model of the Baltic Sea developed by Gustafsson and Savchuk. The model reproduces the major features of observed variations of stratification, nutrients and biogeochemical process rates.

RCO-SCOBI is a high-resolution three-dimensional coupled physical-biogeochemical ocean model of the Baltic Sea developed at SMHI to study environmental issues on long time scales (Eilola et al., 2008; Eilola and Meier, 2006; Marmefelt et al., 1999; Meier et al., 2003; Meier and Kauker, 2003). The model has been used to assess climate variability of the past 100 years and to study the impact of future climate at the end of the 21<sup>st</sup> century on the marine ecosystem.

Both BALTSEM and RCO-SCOBI describe the dynamics of nitrate, ammonium, phosphate, diatoms, flagellates, cyanobacteria, zooplankton, detritus, and oxygen. Silicate is available as an option. The sediment contains nutrients in the form of benthic nitrogen and phosphorus including aggregated process descriptions for oxygen dependent nutrient regeneration, denitrification and adsorption of ammonium to sediment particles, as well as permanent burial of organic matter.

BALTSEM was the main mechanistic model of the MARE program and is now an integral part of the work within the Baltic Nest Institute. RCO-SCOBI has been validated in many publications and is used as a key tool in projects financed by the EU (FP6 and INTERREG) and by national funding agencies, like the Swedish Research Council, the Swedish Governmental Agency for Innovation Systems, the Swedish Environment Protection Agency and the Swedish Research Council for Environment, Agricultural Sciences and Spatial Planning.

Simulations of the following cases were made:

Case 0. Control case without any alterations

- Case 1. Halocline ventilation – the idea put forward by Stigebrandt and Gustafsson (2007) to pump water from 50 to 120 m depth
- Case 2. The salt lock – the idea by the O2-gruppen that is based on regulating flows through the Great Belt ([www.o2gruppen.se](http://www.o2gruppen.se))
- Case 3. Opening/closing of the straits – not really seriously proposed by anyone, but the discussion on the effects of general increasing/decreasing flow capacity of the straits are coming up regularly:
  - Case 3a. Closed Öresund at the Drogden Sill
  - Case 3b. Dredged Drogden Sill to twice the present depth
- Case 4. Deep water oxygenation – supply oxygen to the deep water in sufficient amounts to keep the water from being hypoxic without disturbing stratification

Through model simulations the following consequences of each engineering solution are assessed:

- 1) the magnitude of the disturbance on physical circulation of the Baltic proper
- 2) the change in hypoxia
- 3) the change in plankton biomass and primary production including cyanobacteria, as important indicators of the Baltic Sea eutrophication.
- 4) the change of cod “reproduction” volumes
- 5) the major uncertainties of the projections

The purpose of the simulations at this stage was not to certify whether a specific method works or not, but to reveal key issues and most importantly they served as a concrete basis for discussions at the third workshop “Responses and effects of different engineering solutions on Baltic hypoxia” of the Baltic Sea 2020 project coordinated by Daniel Conley (see [www.balticsea2020.org](http://www.balticsea2020.org)).

One additional outcome from the modeling will be a list of developments necessary for making proper analysis of the consequences of engineering measures. Especially useful in this respect is that we exposed the simulations to criticism and debate that gave us additional input. It could be how to parameterize critical “natural” processes as well as how to correctly implement, for example, ventilating pumps in the models. Depending on this outcome, an application for a second stage may be submitted that includes refinements of model formulations and implementations necessary to produce more definitive recommendations.

This brief report serves as a summary that gives reference to some technical aspects of the model simulations and to the figure material of the results. Basic interpretations of the simulations are made.

## **2 Method**

### **2.1 BALTSEM description and implementation**

#### *2.1.1 Brief model description*

The BALTic sea Long-Term large-Scale Eutrophication Model (BALTSEM) is a coupled physical-biogeochemical model forced by observed meteorology, river runoff and oceanic sea levels. In addition, nutrient loads through river runoff, point sources and atmospheric deposition are fed into the model. The model concept is a time-dependent basin-scale model. The physics was presented in detail by Gustafsson (2000; 2003). The model resolves the Baltic Sea horizontally with thirteen sub-basins (see Figure 2.1.1). Each sub-basin is vertically resolved with variable number of dynamic layers. New layers are formed due to inflows of distinct new water masses, establishment of shallower and less dense surface layer due to heating, or inflow of less dense water. As the number of layers attends a maximal value, the two layers that require the least energy to mix are merged. Water exchanges between basins are parameterized using well-established dynamic laws. The model also features a full air-sea exchange module, including sea ice dynamics.

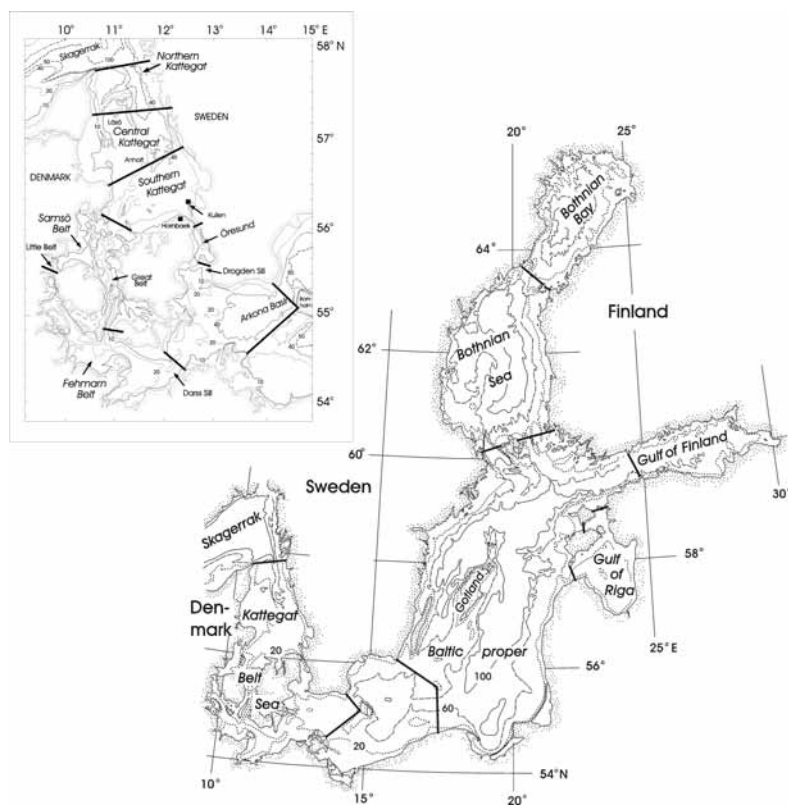


Figure 2.1.1: Map showing the sub-basin boundaries in the BALTSEM.

The biogeochemical processes are directly coupled with the physical model for the sub-basins of the Baltic inside the sills starting with Bornholm basin. The biogeochemical state is described by twelve pelagic state variables: oxygen, ammonia, nitrate, phosphate, silica, nitrogen detritus, phosphorus detritus, silica detritus, cyanobacteria, diatoms, dinoflagellates, and zooplankton. Using the hypsographic function for each basin, the area of bottoms for each depth (with 1 m resolution) can be determined. Three sediment state-variables (benthic nitrogen, phosphorus and silica) are defined at these bottom areas. Thereby sediment water exchange will occur throughout the water depth. In Figure 2.1.2, there is a sketch of the main biogeochemical state variables and fluxes.

The parameterizations of biogeochemical fluxes occurring according to Figure 2.1.2 are mostly the same as presented in detail with relevant references by Savchuk and Wulff (1996, 2001) and Savchuk (2002). Here, we give qualitative description of these parameterizations together with a few modifications required by expansion of the model, initially developed and calibrated for the Baltic Proper and the Gulf of Riga, onto the gulfs of Bothnia and Finland.

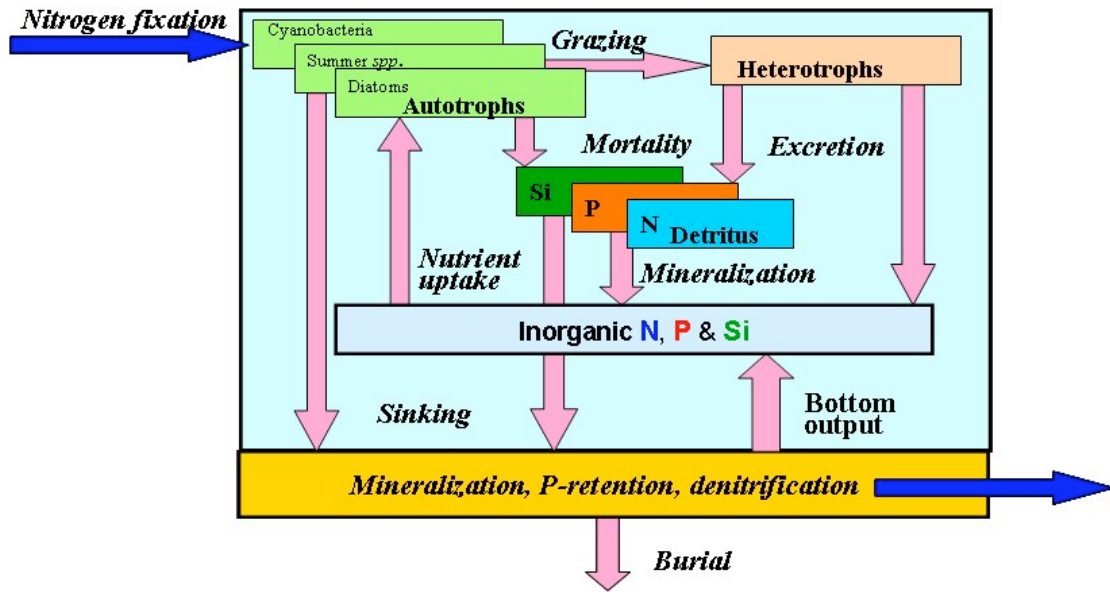


Figure 2.1.2: Sketch of the biogeochemical state variables and fluxes in BALTSEM.

The food consumption by heterotrophs is modeled as a filtration rate, which depends on both temperature and the availability of food consisting of both autotrophs and detrital suspended particles. A part of the consumed food is assimilated, while unassimilated particles are added to the detritus pool. The heterotroph biomass decreases due to mortality and excretion. To mimic the top-down control by higher trophic levels, mortality of heterotrophs is density dependent. The temperature-dependent excretion of ammonium and phosphate by the heterotrophs is used for the coupling and stoichiometric adjustment of the nitrogen and phosphorus cycles. This parameterization accounts for the lower and changing N: P ratio of the ingested food comparing to that of consumers and results in faster recycling of phosphorus comparing to nitrogen.

Light and concentrations of inorganic nutrients control the temperature-dependent growth rate of all autotrophs. Photo-inhibition at high light intensities and a fast adaptation at low levels are included into the parameterization of the light effect. Limiting effects of nutrient concentrations are described by Michaelis-Menten kinetics, the ammonium-induced inhibition of nitrate uptake included. The cyanobacteria are enabled to fix molecular nitrogen when water temperature is higher than 13 – 14 C° and the ambient inorganic N:P molar ratio lower than the Redfield ratio of 16. The nitrogen fixation rate is then dependent on temperature, ambient N:P ratio, and concentration of phosphate. The mortality rate and the sinking velocity of autotrophs are temperature dependent and

inversely related to the same limiting functions that are used to describe the growth rate. Thus, these losses increase when growth limitation occurs.

The detrital nitrogen, phosphorus, and silica concentrations increase due to plankton mortality and decrease by consumption of heterotrophs as well as by temperature-dependent mineralization and sedimentation. The sinking velocity is also proportional to the ratio between detritus silica and nitrogen, to mimic a faster sedimentation of 'diatoms' comparing to other sources of detritus.

Mineralization increases concentrations of ammonium and phosphate. Ammonium is nitrified to nitrate under aerobic conditions. At low oxygen concentration, preformed nitrate is denitrified to molecular nitrogen. This denitrification starts at a "threshold" oxygen concentration and depends on temperature and nitrate concentration.

Oxygen is produced by autotrophs and is subject to exchange with the atmosphere. Oxygen consumption includes terms for heterotroph requirements, mineralization of organic matter including consumption by sediments, and nitrification. Hydrogen sulfide (treated as "negative oxygen") is produced under anaerobic decomposition of organic matter and oxidized when oxygen is present.

Sediment pools of nutrients are increased by sedimentation of autotrophs and detritus and are decreased due to mineralization and burial. To mimic decomposition of the more labile freshly deposited organic matter in summer, the mineralization rates are made dependent on the square of water temperature. Mineralization fluxes are split into several pathways, the proportions depending on water oxygen concentration. One fraction of nitrate produced under aerobic conditions is released into the overlying water and the remaining fraction is denitrified. Under anaerobic conditions the mineralized nitrogen is released as ammonium part of which is adsorbed to sediment particles. Under aerobic conditions one part of phosphate produced is retained (sequestered) in sediments by sorption. The remaining fraction is released into the overlying water. Under anaerobic conditions no adsorption occurs and some of the previously adsorbed phosphorus is released to the water column as well. The phosphorus retention capability of sediments inversely depends on salinity, which is considered an indicator of both the sulfate concentration and the contribution of iron- and humus-enriched fresh waters. All mineralized silica is released into the water. Finally, sediment nutrients are buried with a constant rate.

A downward effective nutrient transport due to resuspension is mimicked by continuously relocating some fraction of benthic nutrient variables from the upper to lower sediment layers. The fraction is assumed to decrease with depth.

### *2.1.2 Forcing and simulation strategy*

The simulations consist of two parts: the base simulation and then the experimental (or forecast) simulation. In the base simulation the model is initialized with observed profiles on Jan 1, 1970 and the model is run with real forcing to Dec 31, 2006. It is assumed that the engineering measure is taken instantaneously on Jan 1, 2007 and a 111 year long forecast simulation with statistical forcing and approximately invariable nutrient loads is started for each measure. A control run, without any engineering measure is also conducted.

For simulation of the base period 1970 – 2006, the forcing is based on actual observations. The driving forces are 3 hourly standard meteorological observations of wind, air temperature, cloudiness, relative humidity, air pressure and precipitation. Additional forcing data are daily sea level as observed in Hornbaek in Kattegat and monthly river runoff. For additional information of the physical model details the reader is referred to Gustafsson (2000; 2003). Monthly loads from rivers, point sources and atmosphere is compiled for the simulation period from information contained in the Baltic Environment Database (BED) maintained at the Stockholm University.

The length of the forcing data set, 37 years, is the same as the residence time for salt in the Baltic Sea (Stigebrandt and Gustafsson, 2003) and model simulations indicate that about 100 years is needed for forcing and salinity to statistically equilibrate (Omstedt and Hansson, 2006). Thus, in order to analyze the statistical equilibrium properties, we would need to simulate at least 100 years. One method is to make use of the same forcing time-series over and over again as done by e.g. Omstedt and Hansson (2006). Another method is that from the available forcing data construct random forcing time-series. The problem is that there is an interrelation between the different forcing variables, e.g., strong winds and high sea level. One method can be to quantify the correlation between the various variables and use the correlation matrix to generate a random, statistically consistent forcing data set. However, here we establish a simple pragmatic solution to construct random forcing data that are consistent. The idea is that the forcing data set is cut in a number of time-slices. These slices are merged into a new continuous time series by

random selection. Care needs to be taken to preserve the seasonal cycle by putting the slices at approximately the same time of the year as in the position of the original forcing time series. A problem is the discontinuities, or abrupt changes, that occur when two slices are put after each other. This is not a major issue for the weather parameters as large changes, in for example wind or temperature, happen during the course of 3 hours naturally and even if rapid change is exaggerated it will not cause problems in a model of this type. The sea level forcing is an exception to this rule, a rapid shift in Kattegat sea level cause large water transport through the Danish straits that can cause significant and long-lasting changes in for example Baltic deep waters. This is solved by cutting the original forcing data set at points when the sea level in Kattegat does a zero crossing and thereby all slices start and end with zero sea level. Using this method, we constructed a 111 yr (3x37 years) long forcing time-series that should have the same statistical properties as the past decades. For nutrient loads, we computed monthly averages of river concentrations, concentrations in rain, and of point sources and dry deposition from the period 2000 – 2003. These averages prevail during the whole 111 year period.

### *2.1.3 Implementation of engineering cases*

Here we describe what modifications that were made into the model to simulate the effects from the engineering measures.

#### *2.1.3.1 Case 1: Halocline ventilation*

Stigebrandt and Gustafsson (2007) proposed that pumping approximately 10 000 m<sup>3</sup>/s of water from 50 to 125 m depth in the Baltic proper would greatly reduce the extent of the hypoxic area, and thereby reduce the internal load of phosphorus. They based their calculations on an order of magnitude estimate of the oxygen consumption and organic matter remineralization in these layers. They made a quantitative estimate that the pumping could be performed by 100 wind forced pumping stations, each pumping 100 m<sup>3</sup>/s through a 7 m in diameter pipe, consuming about 60 MW each including frictional losses and overall efficiency of transmission and pumps of 65%. Efficient initial mixing can be obtained by mounting a properly diffuser at the outflow end of the pipe, but such technical optimizations were beyond the scope of their analysis.

We implemented a sub-model of the action of the pumps and the plumes that form at depth floating upwards. Water is taken from 50 m depth and brought down to 125 m, where it is released as an upward facing plume. An upward plume generate least mixing,

but is easiest to implement. A downward facing plume would cause initially a momentum forced plume reversing into a buoyant upward plume at some distance down. Also one could redirect the momentum radial direction with a diffuser. However, what we want to mimic here is that the mixing process caused by the plume is not the same as Fickian mixing, that is, as the light water plume rises the volume flow increases and buoyancy decreases due to entrainment of ambient water. The plume will settle at a level of neutral buoyancy. The model we use follows Turner (1973). In order to achieve a substantial mixing we had to reduce the tube radius by a factor of two from the values in Stigebrandt and Gustafsson (2007).

#### *2.1.3.2 Case 2: The salt lock*

The idea proposed by the so-called O2-group with participants primarily from KTH in Stockholm comprises a flap-like construction on the sea floor to be placed in the Great Belt. When flows are southward the flap should be pressed to the bottom and thus the channel is fully open and for northward flows the flap will rise and limit the flow of the deeper, more saline layers. The description at the home page of the O2-group does not contain the actual dimensions of the flap, but from the illustrations we have assumed that the depth is reduced to 20% for northward flows. Such narrow constriction will cause additional flow resistance due to the contraction of the flow above the flap. The barotropic flow through the straits is computed using a separate barotropic channel model. We estimate that the flap will cause a reduction of the barotropic transport capacity down to about 60% of the normal. Reduced depth will cause less baroclinic flow, but as the results will show below, the baroclinic component of flow through the Great Belt is small in the BALTSEM.

#### *2.1.3.3 Case 3: Closing and dredging of Drogden Sill*

These are straightforward cases. Closing of Drogden sill implies simply that all flows will go through Great Belt and was easily implemented in the model. Dredging to twice the depth has two consequences: water will be drawn from greater depths in the Öresund and flow capacity will increase due to less friction. The model handles the first effect automatically when depth of the sill is increased, but the increase in flow capacity needs to be estimated separately. The change in flow capacity in a strait due to changes in morphology was described in Gustafsson (2004). It comes out that the flow capacity increases by a factor of  $\sqrt{2}$ .

#### 2.1.3.4 Case 4: Oxygenation

In this case we supply sufficient amount of oxygen to keep concentrations at or above 2 ml/l (2.86 g/m<sup>3</sup>). This is done in practice by introducing an artificial source term in the oxygen conservation equations that is zero if concentration is above 2 ml/l and equal to  $(2 - C_{O_2})/DT$  if concentration ( $C_{O_2}$ ) is below 2 ml/l ( $DT$  is the time-step).

## 2.2 RCO-SCOBI description and implementation

The model system is based on the Swedish Coastal and Ocean Biogeochemical model (SCOBI) (Eilola et al., 2008; Marmefelt et al., 1999) and the Rossby Centre Ocean circulation model (RCO) (Meier et al., 2003; Meier and Kauker, 2003). The model domain of the RCO-SCOBI model covers the Baltic Sea including the Kattegat (Fig. 2.2.1) with a 6 nm horizontal resolution and a maximum depth of 250 m in the present set-up. The vertical resolution of the model is 41 levels with an increasing layer thickness from 3 m in the surface layers to 12 m in the deep Baltic Sea.

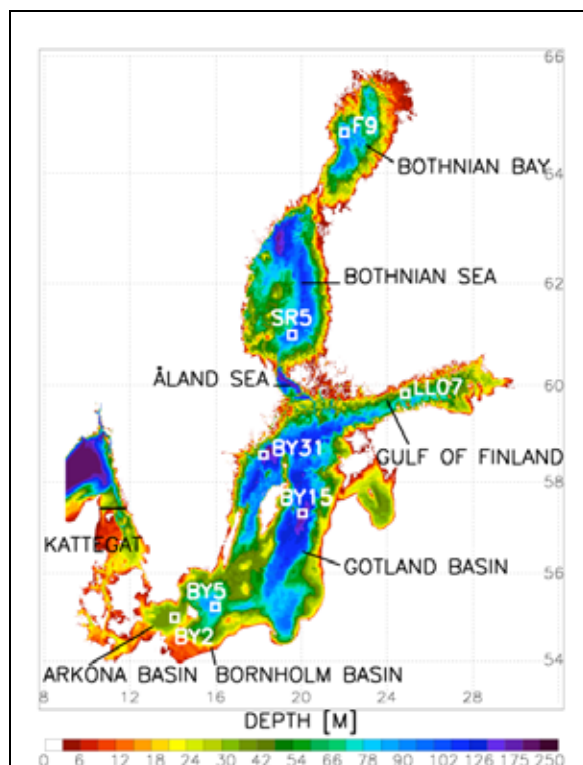


Figure 2.2.1. Overview of the model domain. The black line indicates the open boundary in the northern Kattegat. The color bar shows depths in meter. Monitoring stations used for model validation are indicated by white squares.

The one-dimensional SCOB1 model is in each grid point coupled by means of advection and diffusion equations for the biogeochemical state variables to the latest version of the high-resolution RCO model (Meier, 2007). In each time step, first the changes due to physical transports (advection, diffusion, open boundary exchange) and exchanges with the atmosphere (air-sea oxygen fluxes, nutrient deposition) and land (nutrient loading from river runoff including diffuse and point sources) are computed. Thereafter changes due to biogeochemical sources and sinks are explicitly computed. Benthic variables are not affected by the physical transport system and are handled by the SCOB1 model alone.

### *2.2.1 The RCO model*

RCO is a Bryan-Cox-Semtner primitive equation circulation model with a free surface and open boundary conditions in the northern Kattegat. It is coupled to a Hibler-type sea ice model with elastic-viscous-plastic rheology. Subgrid-scale mixing is parameterized using a turbulence closure scheme of the  $k-\epsilon$  type with flux boundary conditions to include the effect of a turbulence enhanced layer due to breaking surface gravity waves and a parameterization for breaking internal waves. The deep water mixing is assumed to be inversely proportional to the Brunt-Väisälä frequency. A bottom boundary layer model is used to simulate gravity-driven dense bottom flows and a flux-corrected transport scheme is used to guarantee the numerical stability of the RCO model. No explicit horizontal diffusion is applied. For further details the reader is referred to Meier et al. (2003).

#### *2.2.1.1 Model forcing and setup*

Previous investigations showed that it is necessary to have long spin-up times both for the physical model and for the biogeochemical model. The mean ages of inflowing Kattegat water varies from about 10 years in the Arkona deep water to more than 40 years in the northern Baltic surface waters (Meier, 2007). RCO was therefore started from rest with initial temperature and salinity observations from November 1902. A spin-up was run with reconstructed atmospheric forcing and river discharge data till the end of 1998 (Kauker and Meier, 2003). The biogeochemical variables of the SCOB1 model were initiated with realistic profiles that are assumed to represent the entire domain. The results from the end of the spin-up were used as initial conditions for the simulations presented here. The analysis of the results covers the last 30 years of the simulation period (1969-1998).

Average atmospheric nitrogen deposition was computed from estimates for every 5<sup>th</sup> year of the period 1980-2000 and distributed over the surface areas of 6 sub-basins, the

Bothnian Bay, the Bothnian Sea including the Åland Archipelago Sea, the Gulf of Finland, the Gulf of Riga, the Baltic proper including the Bornholm and Arkona basins, and the Kattegat including the Danish straits, the Belt seas and the Sound. Atmospheric phosphorus deposition was based on a constant value from Areskoug (1993). The rivers in the RCO model include the 30 most important coastal segments of the Baltic Sea and incorporate all freshwater runoff and nutrient supplies from land to the sea. The climatological (1970-2000) monthly mean nutrient concentrations of the rivers were mainly based on the data set collected by Stålnacke et al. (1999). Atmospheric and river data were extracted from the Baltic Environmental Database (BED) via the internet based information environment for decision support system NEST (<http://nest.su.se/nest/>). Averaged point sources of municipal and industrial discharges (HELCOM, 1993; 1998; 2004) were computed from 1990, 1995 and 2000 for each country and divided equally between national rivers in each basin. 50% of the total supply was assumed organic for both N and P.

The nutrient supply includes all inorganic nutrients and 75% of the organic phosphorus ( $\text{orgP}=\text{TotP}-\text{DIP}$ ) and about 30% of the organic nitrogen ( $\text{orgN}=\text{TotN}-\text{DIN}$ ). These fractions of the river borne organic nutrients are considered biologically available in accordance with e.g. Stephanousakas et al. (2002). The rest is considered not biologically available and is not incorporated in the present model set-up. The phosphorus supply from rivers to the model varies from about 19 000 ton year<sup>-1</sup> to 34 000 ton year<sup>-1</sup> and the nitrogen supply varies from about 364 000 ton year<sup>-1</sup> to 632 000 ton year<sup>-1</sup>. The 10-year running mean shows a periodicity of about 28 years due to varying river runoff during the period 1902-1998. The nutrient supply from the atmosphere and point sources are constant.

The open boundary conditions in the northern Kattegat were based on profiles of climatological (1980-2000) seasonal mean nutrient concentrations from the station Å17 in the eastern Skagerrak (data from the Swedish Oceanographic Data Centre (SHARK) at the Swedish Meteorological and Hydrological Institute, see <http://www.smhi.se>). The organic nutrient supply was estimated from the difference between total phosphorus and dissolved inorganic phosphorus (TotP-DIP). The bioavailable fraction of this (assumed 75% in accordance with the phosphorus supply from land runoff) was added as particulate detritus to the model. Organic nitrogen was implicitly added because of the Redfield ratio of model detritus.

### 2.2.2 *The SCOBI model*

The SCOBI model (Fig. 2.2.2) contains inorganic nutrients, nitrate ( $\text{NO}_3$ ), ammonium ( $\text{NH}_4$ ) and phosphate ( $\text{PO}_4$ ). Primary production driven by solar radiation assimilates these nutrients by three functional groups of autotrophs, diatoms (A1), flagellates (A2) and cyanobacteria (A3). The vertical light attenuation depends on a background attenuation and attenuation due to varying concentrations of autotrophs in the model. The autotrophs differ by the growth and sinking rates giving each group different characteristics depending on the physical and chemical conditions in the water. The grazing pressure from zooplankton (ZOO) on the autotrophs and on detritus (DET) also differs between the groups. Besides the possibility to assimilate inorganic nutrients the modeled cyanobacteria also has the ability to fix molecular nitrogen ( $\text{N}_2$ ) which may constitute an external nitrogen source for the model system. Hence, cyanobacteria may continue to grow when inorganic nitrogen is exhausted if excess phosphorus is available in the water. Production of zooplankton faeces and predation on zooplankton produces particulate organic matter that together with dead autotrophs adds up to the pool of detritus in the model. Decomposition of detritus as well as excretion of nutrients from zooplankton and predator activities produces nutrients in its mineralized forms  $\text{NH}_4$  and  $\text{PO}_4$ . Diatoms, flagellates and detritus may sink to lower layers or add to the sediment department while cyanobacteria are neutrally buoyant in the model (zero sinking speed). The net sinking velocity of the particles also depends on the vertical movement of the surrounding water.

Carbon (C) is used as the constituent representing detritus and zooplankton. Autotrophs are represented by chlorophyll (Chl) according to a constant carbon to chlorophyll ratio C:Chl. The nitrogen (N) and phosphorus (P) content of autotrophs, zooplankton and detritus are described by the Redfield molar ratio (C:N:P=106:16:1).

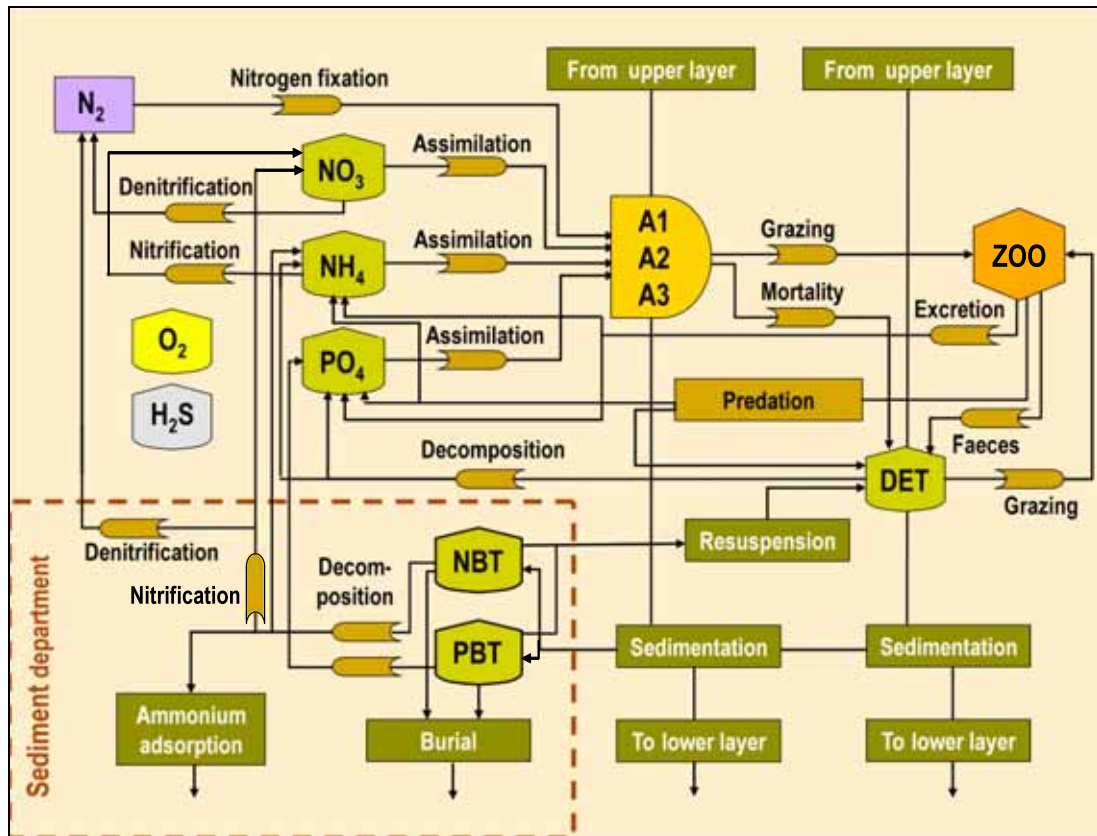


Figure 2.2.2. The SCOB model. Sediment variables and processes are shown in the lower left frame. Note that in the figure the process descriptions of oxygen and hydrogen sulfide are simplified for clarity.

Air-Sea exchange of oxygen ( $O_2$ ) is calculated using wind and temperature dependent exchange rates and temperature and salinity dependent oxygen solubility in sea water. The effects of super saturation due to injection of air bubbles are also included. Oxygen is produced by the autotrophic primary producers and consumed by pelagic and benthic decomposition of organic matter. Oxygen is also consumed by zooplankton and predator respiration and by pelagic and benthic nitrifying bacteria which oxidize ammonium to nitrate.

The sediment contains nutrients in the form of benthic nitrogen (NBT) and phosphorus (PBT). The sediment module includes aggregated process descriptions for oxygen dependent nutrient regeneration, denitrification and adsorption of ammonium to sediment particles. When the bottom stress exceeds critical values, the sinking organic matter stay suspended in the bottom water and re-suspension from the sediments to the overlying water occurs. A fraction of the sediment pools of nutrients is continuously removed from the biochemical cycling by permanent burial in the sediments left below the upper active sediment layer. The quantitative importance of the removal of nitrogen through anaerobic

oxidation of ammonium with nitrite to  $N_2$  (ANAMMOX) in the Baltic Sea is still uncertain (Kiiirikki et al., 2006). This process is not explicitly described but might for now be regarded as included in the denitrification processes of the model.

Pelagic decomposition of organic matter by anaerobic bacteria (denitrification) takes place if nitrate is available when the oxygen concentration drops below about  $1 \text{ mlO}_2 \text{ l}^{-1}$  in the water. Pelagic decomposition of organic matter under anoxic conditions ( $O_2 \leq 0 \text{ mlO}_2 \text{ l}^{-1}$ ) is first carried out by denitrifying bacteria until nitrate is depleted, and then by sulfate reducing bacteria, which produce hydrogen sulfide ( $H_2S$ ) that is included as negative oxygen in the model. Benthic decomposition of organic matter is partly carried out by denitrifying bacteria also when oxygen is abundant in the overlying water. The denitrified fraction increases for declining oxygen concentrations. Benthic decomposition of organic matter under anoxic conditions is first carried out by denitrifying bacteria until nitrate in the overlying water is depleted, and then by the sulfate reducing bacteria. About half of the inorganic nitrogen (ammonium) produced in the sediments under anoxic conditions in the water is removed permanently from the biochemical cycling by adsorption to sediment particles. An oxygen dependent fraction of the mineralized phosphorus in the sediments is adsorbed to sediment particles while the rest is released as a flux of phosphate to the overlying water. The phosphate adsorption process may however reverse when the water turns anoxic and no adsorption occurs. Then some of the previously adsorbed phosphorus may also be released and added to the flux of mineralized phosphorus to the overlying water.

### *2.2.3 Implementation of engineering cases*

In RCO-SCOBI the same engineering cases as in BALTSEM were implemented. However, as RCO-SCOBI is a three-dimensional circulation model, the implementation of the selected cases differs in detail.

#### *2.2.3.1 Case 1: Halocline ventilation*

The halocline in the Baltic proper is ventilated by increased deep water mixing corresponding to an additional energy supply of 600 MW. The Baltic proper comprises the Bornholm Basin east of the island Bornholm and the entire Gotland Basin south of the Åland Sea and the Finnish Archipelago Sea. The Gulf of Finland and the Gulf of Riga are not included. The additional mixing is applied in a depth interval between 61 and 124 m and horizontally homogeneous. In RCO-SCOBI the deep water mixing is parameterized

by an additional term in the k- $\epsilon$  turbulence model which is inversely proportional to the Brunt-Väisälä-frequency. We add the additional mixing power from the suggested pumping stations to this term.

#### *2.2.3.2 Case 2: The salt lock*

The salt lock is implemented in the Great Belt between Nyborg and Korsör. When the vertical integrated transport of any individual grid point at the position of the salt lock is going southward, the flow is not altered. However, when the vertical integrated transport is northward directed, the currents between 6 m and the bottom are set to zero. Consequently, the integrated volume flow above the lock is reduced by the fraction of 6 m to the local water depth.

#### *2.2.3.3 Case 3: Closing and dredging of Drogden Sill*

Closing and dredging of the Drogden Sill is easy to implement and does not affect the source code of RCO-SCOBI. In Case 3a the Öresund at the Drogden Sill is closed. In Case 3b the depth of the Öresund is set to twice the observed depth. An additional Case 3x is performed to illustrate the increased salt flow through both straits – the Great Belt and the Sound – when the salinity distribution of the inflowing water does approximately not change. The salt flux is increased by increasing the sea level amplitude at the open boundary in the northern Kattegat by 30%.

#### *2.2.3.4 Case 4: Oxygenation*

In this case a sufficient amount of oxygen is supplied to keep the oxygen concentrations of the bottom grid cells above the critical threshold of 2 ml/l. The oxygen concentration is just set to the critical value if the concentration is below the threshold. The oxygen supply is an artificial source term and is stored for book keeping purposes.

### **3 Results**

#### **3.1 Change in salinity and temperature in the Baltic proper**

In Figures 3.1.1 and 3.1.2, the average salinity and temperature profiles from Eastern Gotland basin in central Baltic proper for the last 30 years of the simulations are drawn. The corresponding time-depth plots are shown in Figures 3.1.3 – 3.1.6.

Halocline ventilation (Case 1) does not change surface salinity and temperature, but salinity is reduced with about 1 at 100 meter depth and less than 1 at greater depths. Temperature is also lowered somewhat at depth. The changes are within or just outside natural variability as substantiated by comparing with the variability in Case 0 (see shaded area in Fig 3.1.2).

Implementing the salt lock (Case 2), the models give different response, in the BALTSEM simulation surface salinity in Baltic proper is reduced by 1-1.5 while in the RCO-SCOBI simulation the surface salinity increase with about 4. These results seem to be robust in both models. RCO simulations with 2 nautical mile resolution show similar results as for 6 nautical miles, while sensitivity test with BALTSEM gives lowered salinities for a wide range of reduced strait depths (to 10% - 50% of the original depth). The most probable explanation is that the flow through the Great Belt is quite well mixed giving only a weak baroclinic component in BALTSEM. There is a major difference in the models in that RCO also takes into account sea level dynamics in Kattegat and the Arkona basin, while BALTSEM imposes the same sea level difference between Kattegat and the Arkona for both straits. Thus, the salt lock may induce a circulation around the Danish islands between Öresund and Great Belt that could be captured by RCO but not by BALTSEM.

Both models predict reduced salinities when the Öresund is closed at the Drogden sill (Case 3a), but the magnitudes differ substantially. Surface salinity in the Baltic proper decreases by about 2 in BALTSEM and about 5 in RCO. The salinity reduction is larger at depth, as would be expected, with decreased stability as a consequence. The reduced salinities at depth are accompanied with reduced temperature. The salinity dynamics (Fig. 3.1.3 and Fig. 3.1.5) shows that an initial stagnation period occurs after the Drogden is closed. Because of the stronger response in RCO, the length of this stagnation period is much longer in the RCO simulation than in the BALTSEM simulation.

As expected, deepening of the Drogden sill (Case 3b), results in higher salinities in both models results. In this case the difference in sensitivity is even larger between the RCO

results, that show an increase of the Baltic proper surface (deep water) salinity of about 10 (14), and BALTSEM results that show an increase of only about 1.5 (2.5). In both models the changes lead to stronger stratification and higher deep-water temperatures.

The differing results of manipulations in the Danish straits call for further investigations of the dynamics in this region.

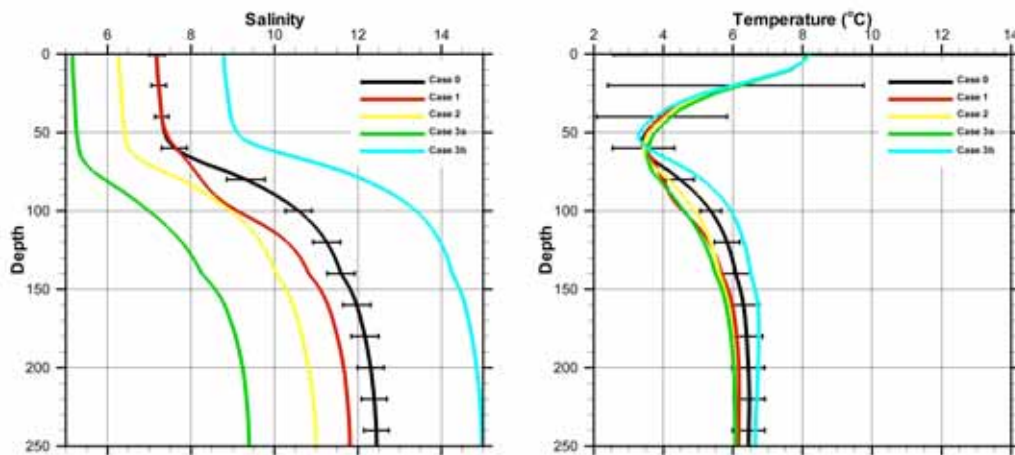


Figure 3.1.1: Average profiles of salinity and temperature for the Baltic proper from the BALTSEM. The averages are computed for the last 30 years of the simulations. Error bars indicate the range of plus to minus one standard deviation.

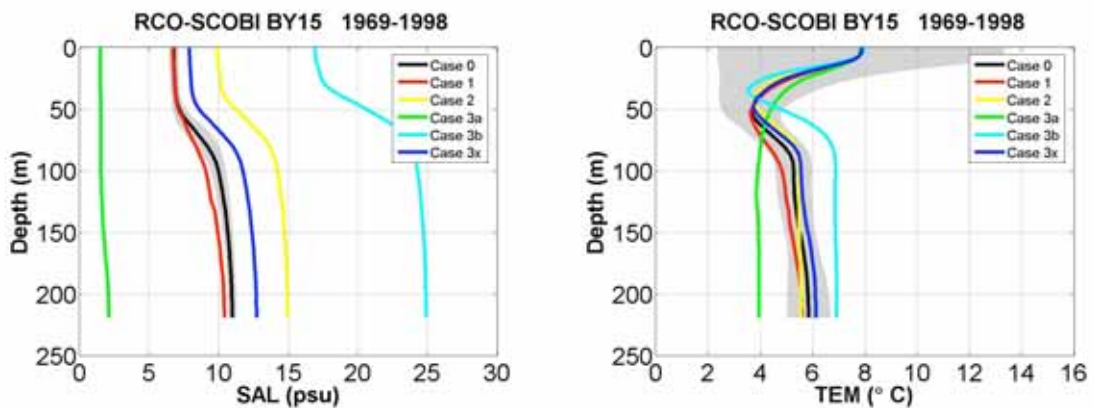


Figure 3.1.2: 30-year average profiles of salinity and temperature at BY15 from RCO-SCOBI. The grey shaded area denotes the range of plus minus one standard deviation.

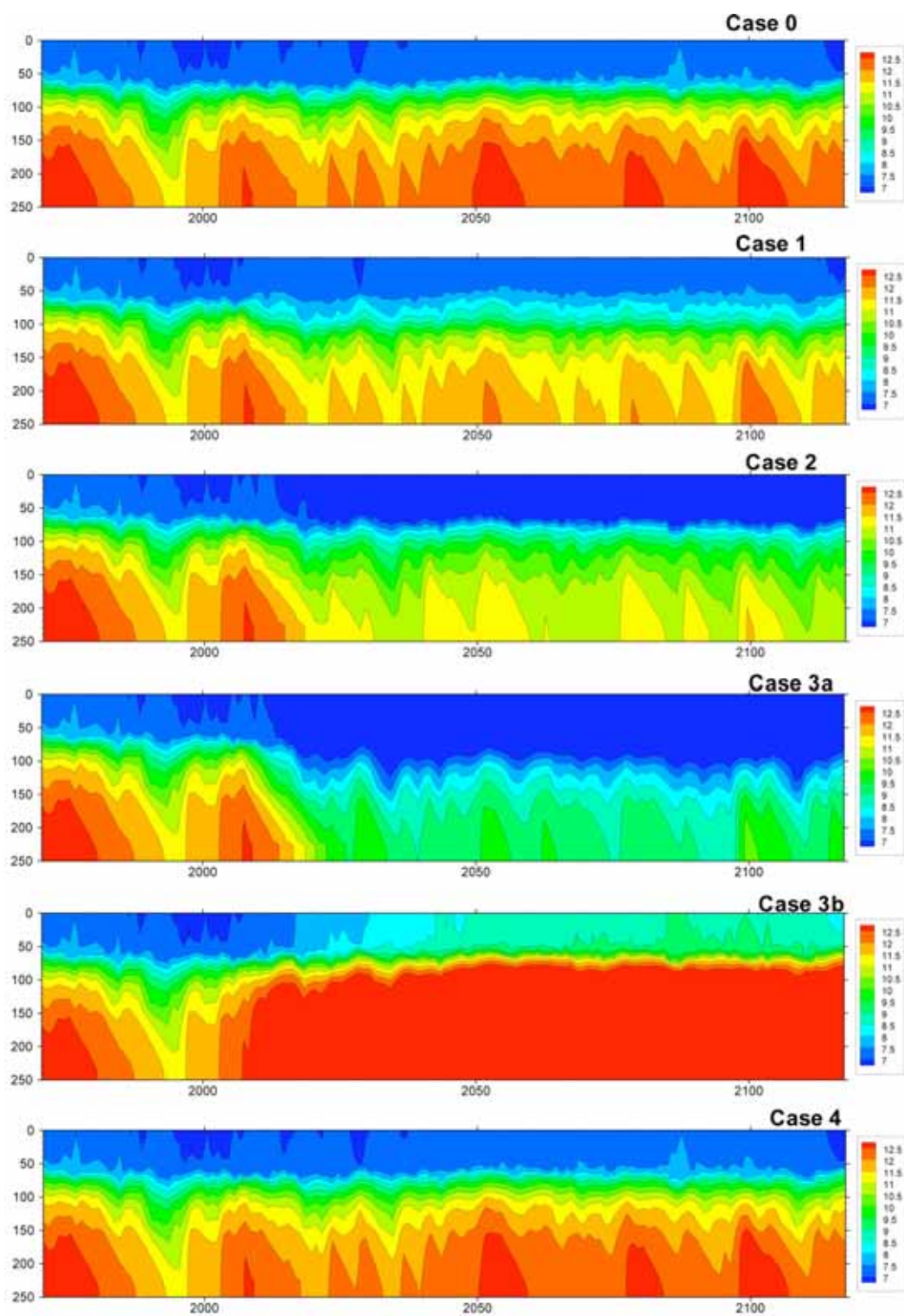


Figure 3.1.3: Salinity as function of depth and time in the Baltic proper for all simulations with BALTSEM. Note that the period up to 2006 is the same for all simulations and that Case 4 does not involve changes in physics.

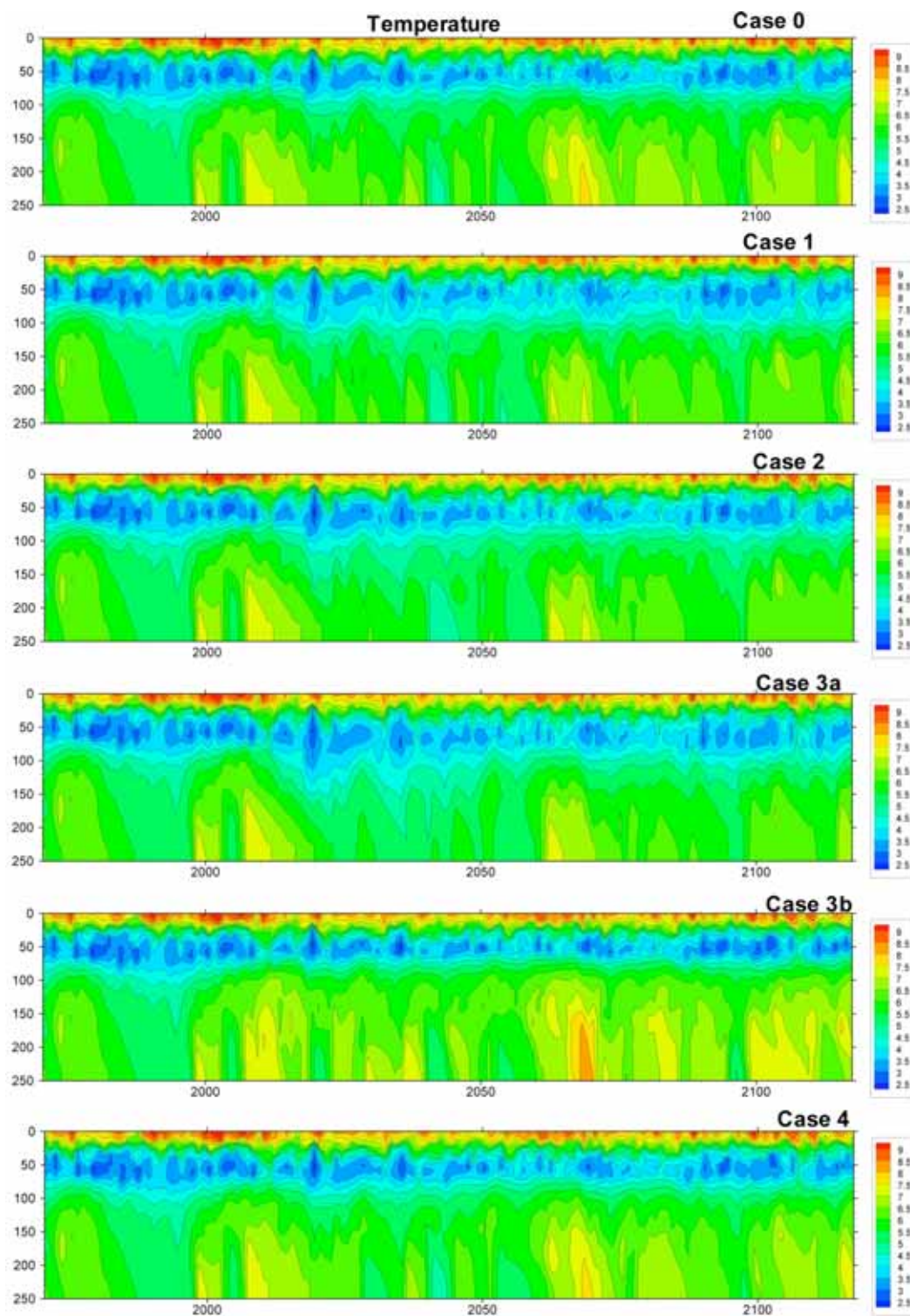


Figure 3.1.4: Temperature as function of depth and time in the Baltic proper for all simulations with BALTSEM. Note that the period up to 2006 is the same for all simulations and that Case 4 does not involve changes in physics.

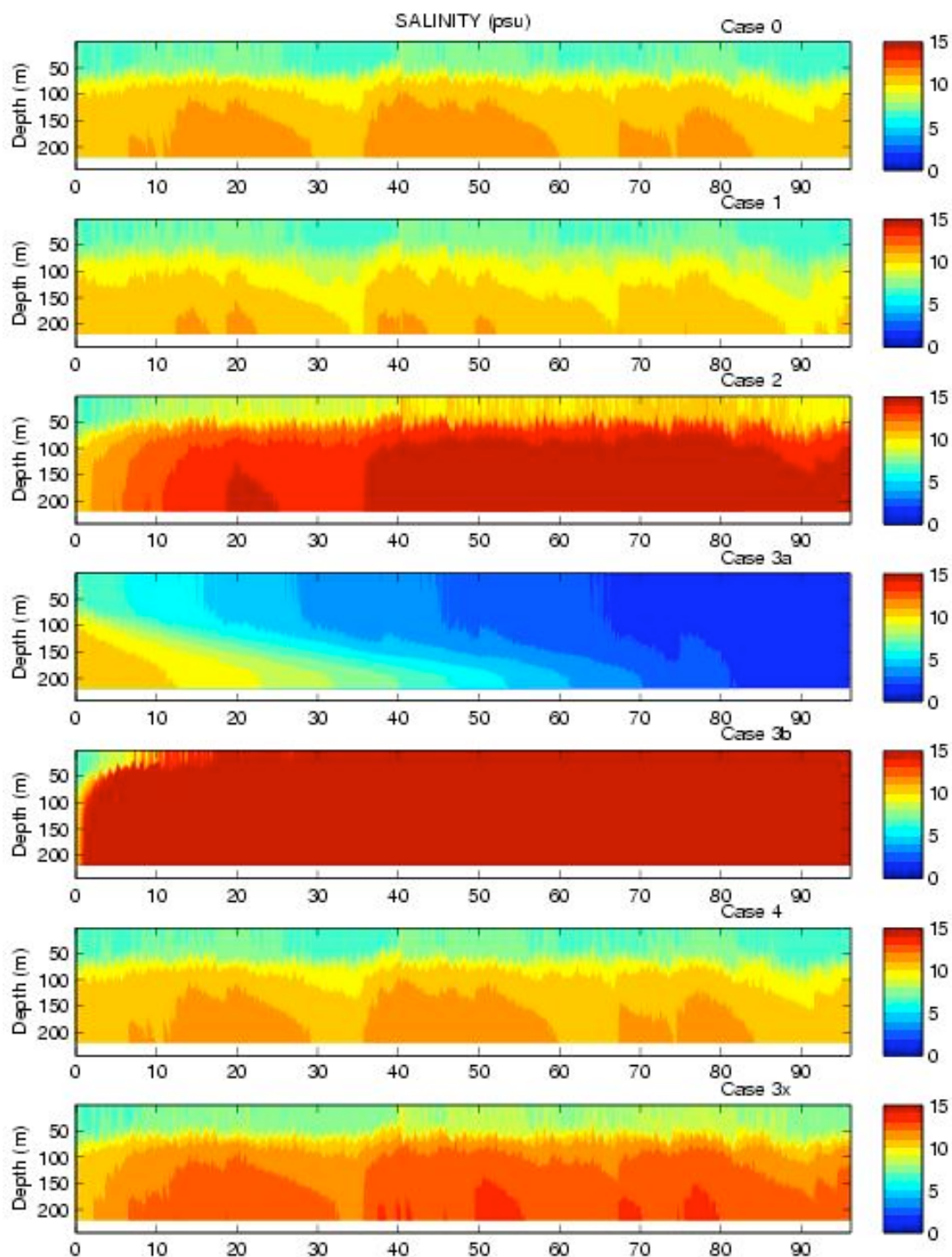


Figure 3.1.5 Salinity as function of depth and time in the Baltic proper (BY 15) for all simulations with RCO. Implementation of the engineering measure is done at year 0 and the model forcing corresponds to the period 1902 - 1998.

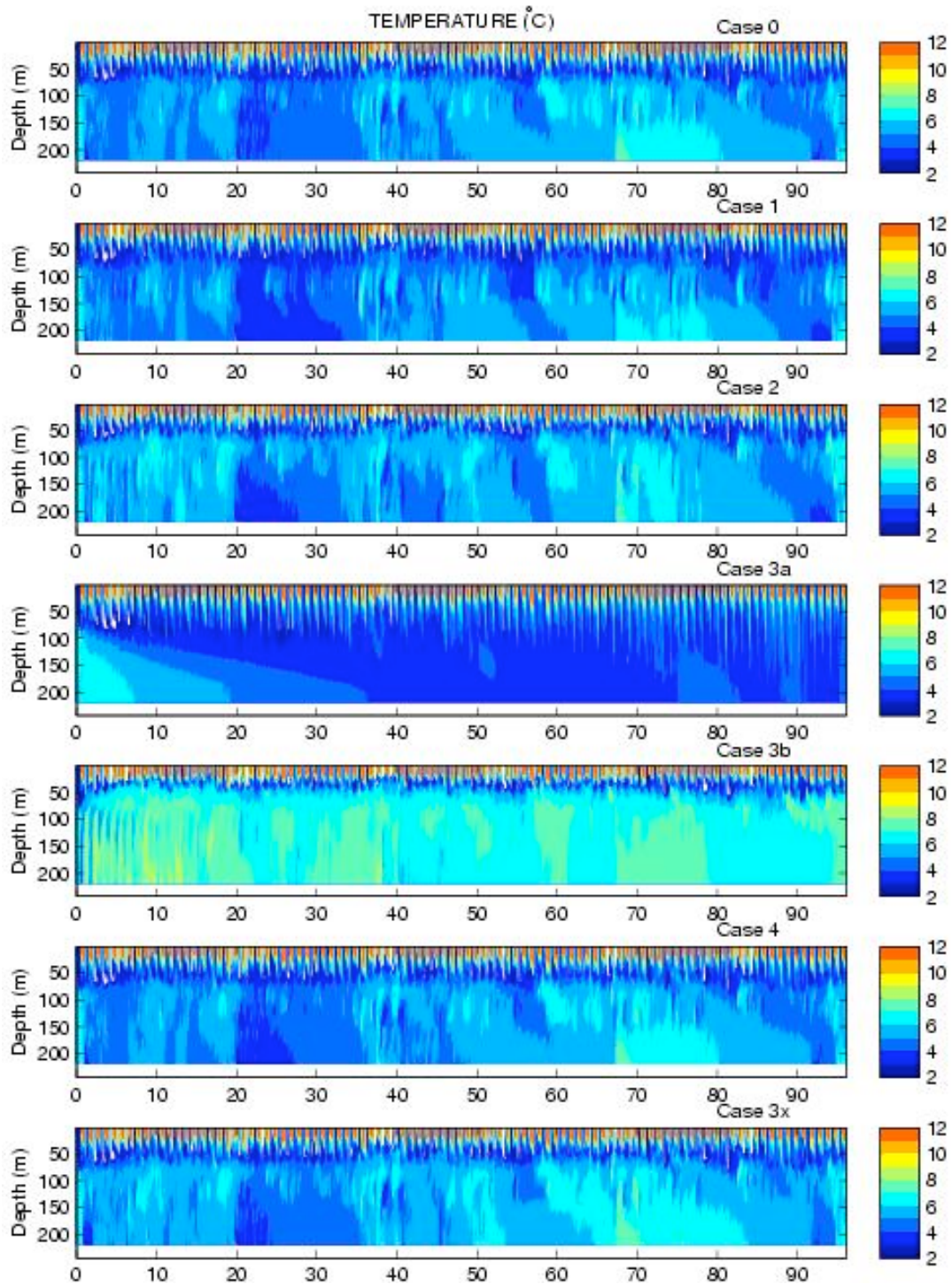


Figure 3.1.6: Temperature as function of depth and time in the Baltic proper (BY 15) for all simulations with RCO.

### 3.2 Change of oxygen and pelagic nutrient concentrations in the Baltic proper

In Figures 3.2.1 and 3.2.2, the 30-year averaged profiles of nutrients and oxygen from the BALTSEM and RCO-SCOBI models are shown. Time-depth plots are presented in Figures 3.2.3 – 3.2.10. The oxygen concentrations are much lower in general in the BALTSEM simulations than in the RCO-SCOBI simulations. The oxygen conditions in

the Case 0 simulation with BALTSEM continue to deteriorate during the reference simulation compared to present day conditions (Figure 3.2.3), indicating that the model initial conditions are not in balance with present loads. Thus, not only inherent model differences but also different simulation strategies made the Case 0 results somewhat different between BALTSEM and RCO-SCOB1 simulations.

Case 4 shows the response of the models to oxygenation of the hypoxic/anoxic waters without changing physical circulation. Thus, it shows the response of the biogeochemical processes alone to redox alterations. Therefore, we present the results from Case 4 first. The RCO-SCOB1 simulations result in this case to a strong phosphorus limitation and a large increase in DIN concentrations. The effect is less pronounced in BALTSEM results. The changes of the phosphate concentrations are small. Although deep-water DIN concentrations decreased, the availability of DIN for production increased due to higher concentrations at intermediate depths. This is confirmed below where we show that primary production is reduced by only a minor fraction, but nitrogen fixation reduces with about 12%.

In Case 1, the halocline ventilation, oxygen concentrations increase in both models results. The increase is larger in BALTSEM simulations with a maximal increase of about 4 ml/l at 100 m compared to about 2 ml/l in RCO-SCOB1 simulations. In the BALTSEM results the deepest layers are still anoxic but halocline ventilation lowers the redoxcline from about 90 to 160 m depth, thus greatly reducing the total bottom areas and water volumes enveloped by anoxia. In both models phosphate concentrations of the deep water are reduced. However the concentrations above the halocline do not change in BALTSEM opposing to a significant decrease in RCO-SCOB1. Given the results from Case 4, it is probable that most of the changes in BALTSEM phosphate concentrations are due to more mixing of low phosphate surface waters into the deep water. There is a tremendous change in DIN in the RCO-SCOB1 results, with higher concentrations from top to bottom. The response in BALTSEM is quite different, there is no change in concentrations above the halocline, a small increase within the upper part of the halocline and decrease from about 100 m to the bottom.

As mentioned above, the results gave differing results as to the circulation in Case 2, the salt lock, BALTSEM results being fresher and RCO-SCOB1 results saltier than Case 0. The biogeochemical models react in response to the circulation change and therefore there

results from the two models are quite different. The BALTSEM indicate improved oxygen concentrations and reduced inorganic nutrient concentrations in the deep, while RCO-SCOB1 show higher phosphate concentrations and somewhat lower oxygen concentrations.

Case 3a, representing a closing of the Drogden sill, results in a fresher Baltic. In both models freshening results in increased efficiency of phosphorus burial due to a salinity dependent parameterization. In BALTSEM results the decrease in DIP is more modest than in RCO-SCOB1 results as a consequence of the salinity changes. The effect on DIN is opposing in the model results, RCO-SCOB1 shows a large increase in DIN indicating a strong phosphate limitation while BALTSEM shows virtually no change in surface concentrations and decreased concentrations apart from a layer between 70 and 100 m. This difference could in parts be explained by the difference in oxygen concentrations and partly by the difference in degree of phosphorus limitation. Case 3b results in decreased oxygen concentrations in both models results. Increase of anoxic/hypoxic areas is further strengthened by a shallower halocline. In addition, the increased salinities cause the salinity dependent phosphorus burial efficiency to decrease which results in increased phosphate concentrations throughout the water column. Also in this case the simulations show different response of DIN concentrations in the deep, they increase significantly in BALTSEM results and decrease somewhat in RCO-SCOB1 results. However, both models results show increased DIN concentrations within the halocline. The reason for different responses may also here be due to the different overall level of oxygen concentrations in the deep. In this case oxygen concentrations from the RCO-SCOB1 simulations at some 80 - 130 m depth change from being at about the limit of hypoxia to clearly hypoxic, while the BALTSEM simulations are anoxic already in Case 0 in this depth interval.

Simulation of some engineering measures aiming at reducing effects from eutrophication of the Baltic Sea

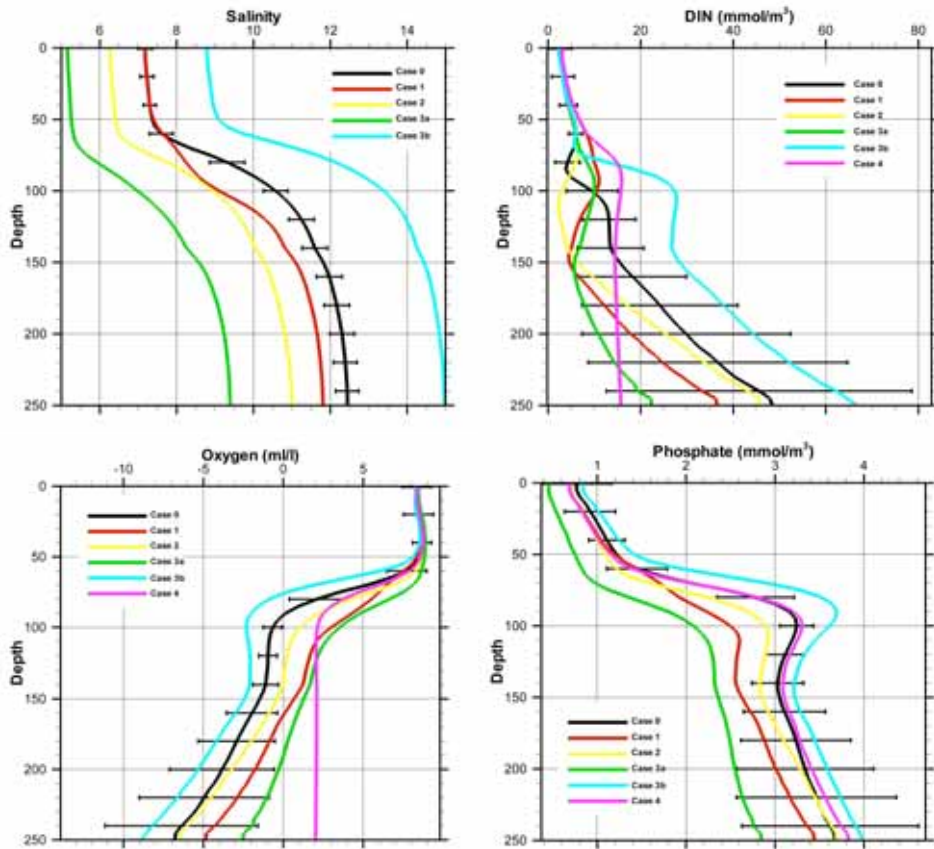


Figure 3.2.1: 30-year averaged profiles of nutrients and oxygen for the Baltic proper from the BALTSEM simulations. The error bars represent the range of variability in Case 0.

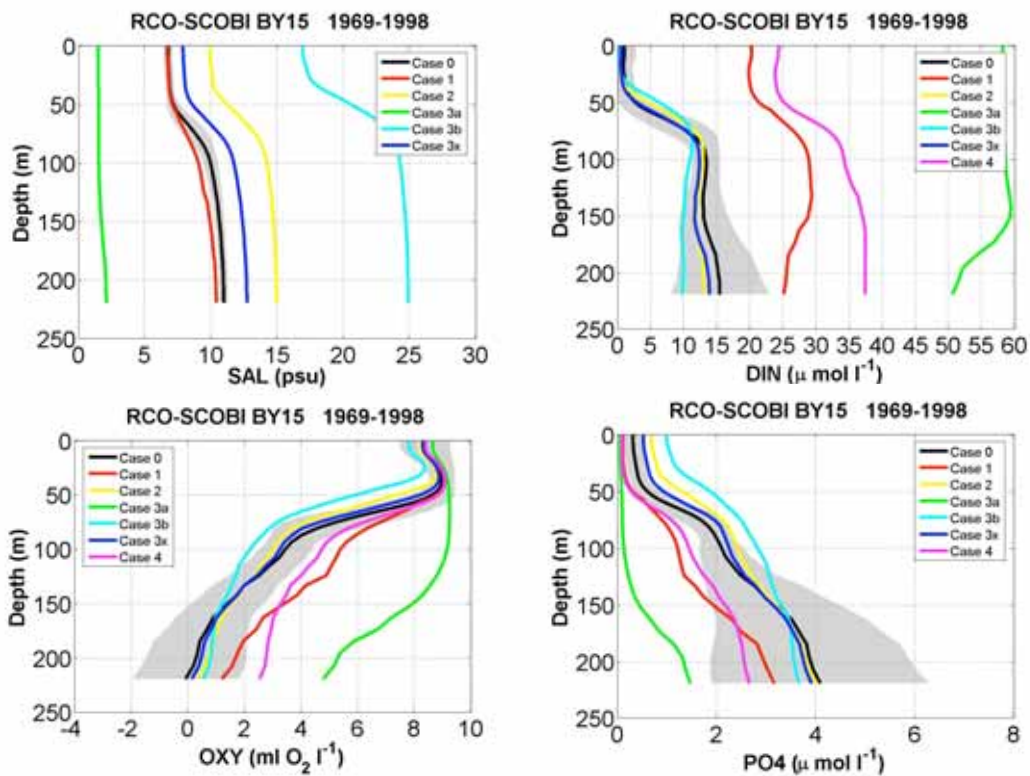


Figure 3.2.2 30-year averaged profiles of nutrients and oxygen for the Baltic proper (Eastern Gotland deep) from the RCO-SCOBI simulations. Shaded area represents the range of variability in Case 0.

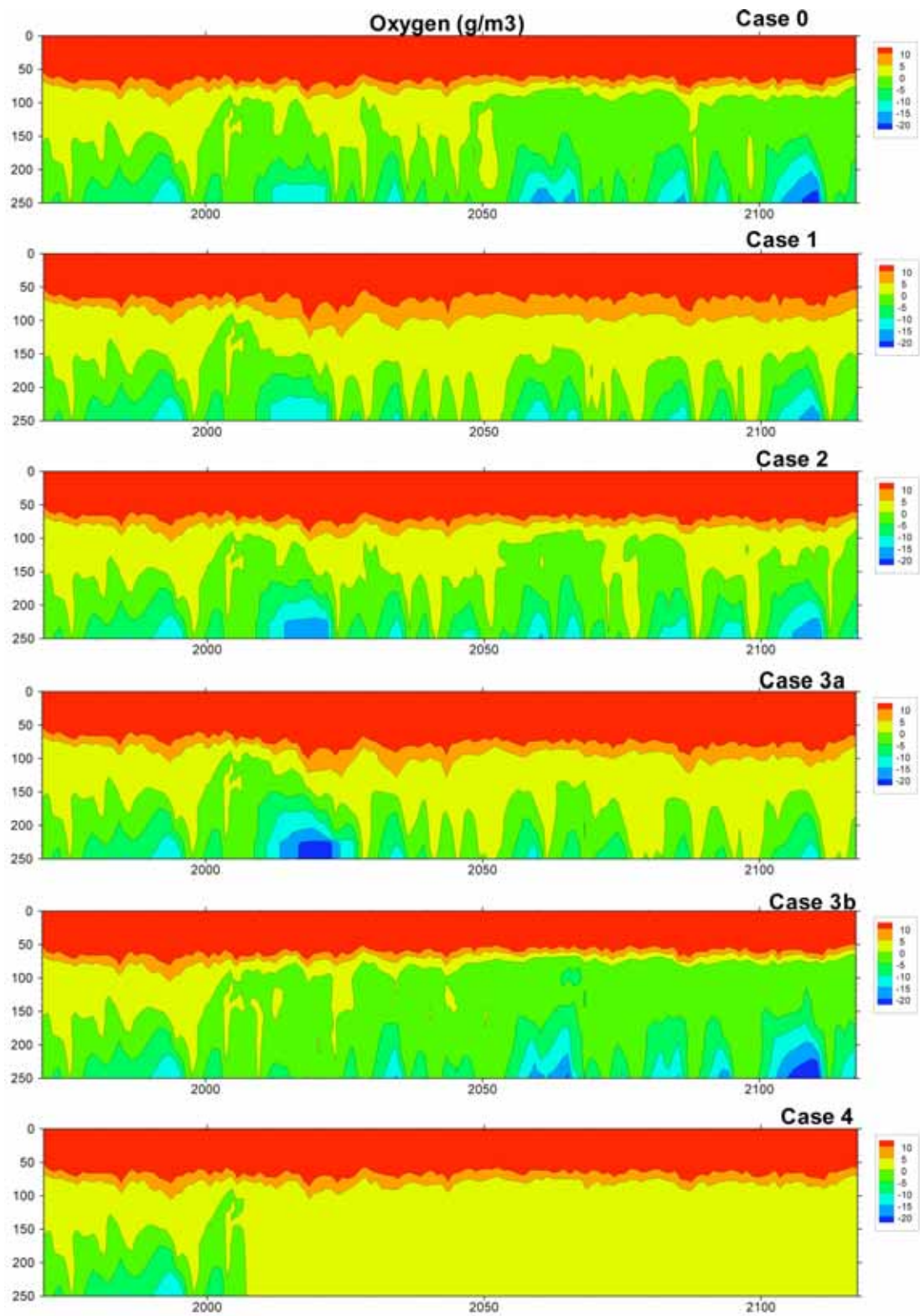


Figure 3.2.3: Temporal development of oxygen concentrations in the Baltic proper from the BALTSEM. Note that the period 1970-2006 was run without manipulations and with realistic forcing and thus is the same for all cases.

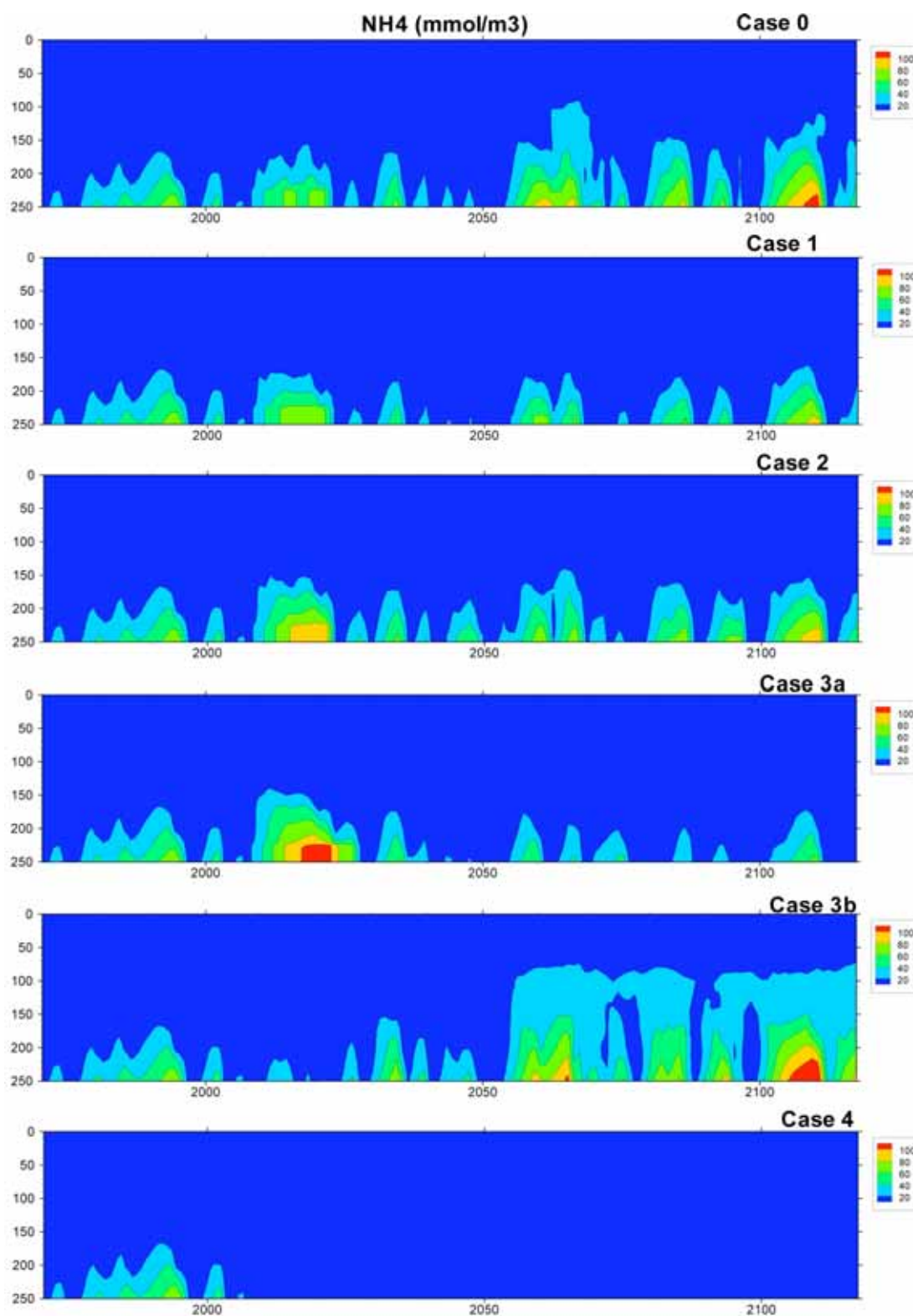


Figure 3.2.4: Temporal development of ammonia in Baltic proper from the BALTSEM simulations.

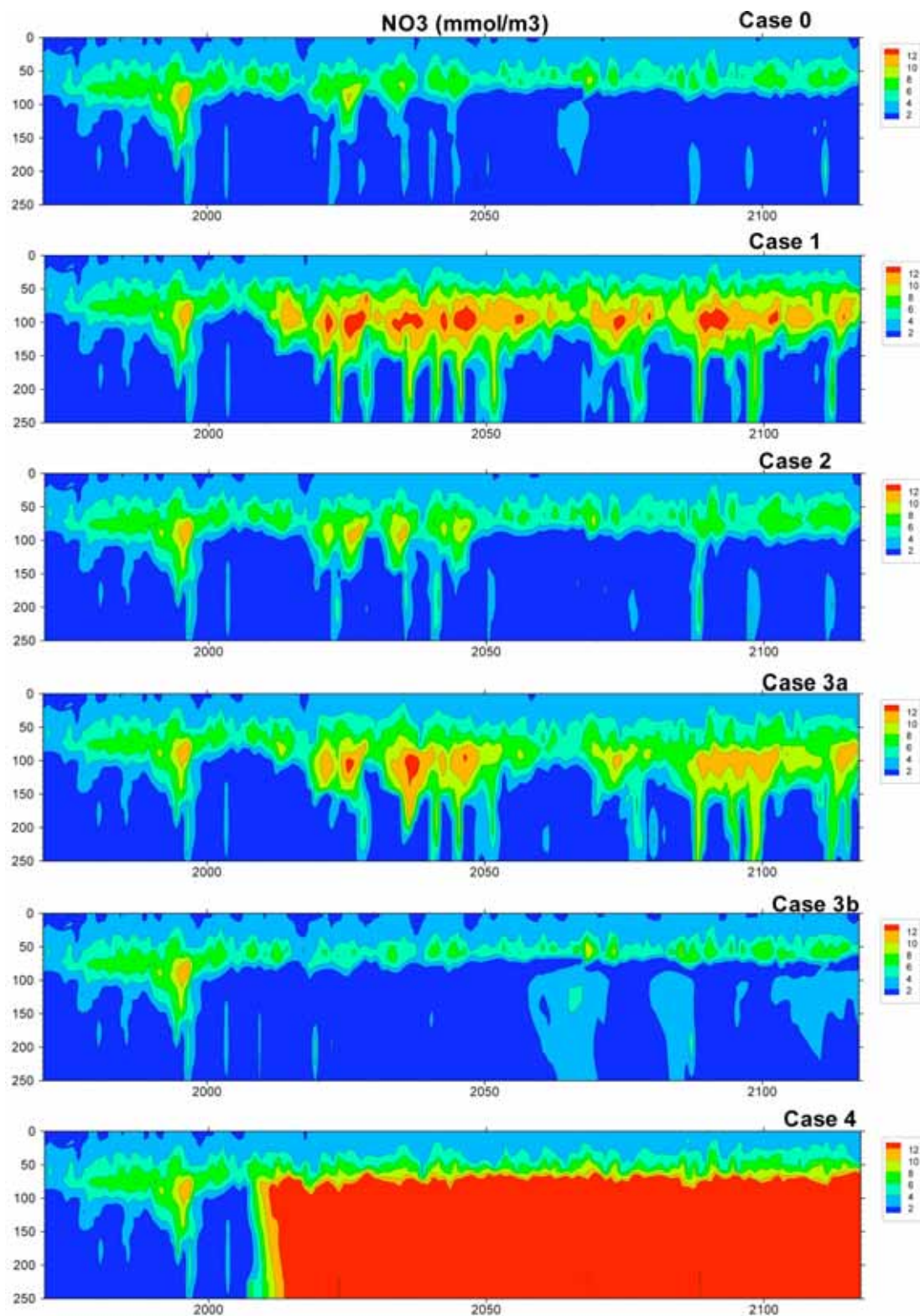


Figure 3.2.5: Temporal development of nitrate in the Baltic proper from the BALTSEM simulations.

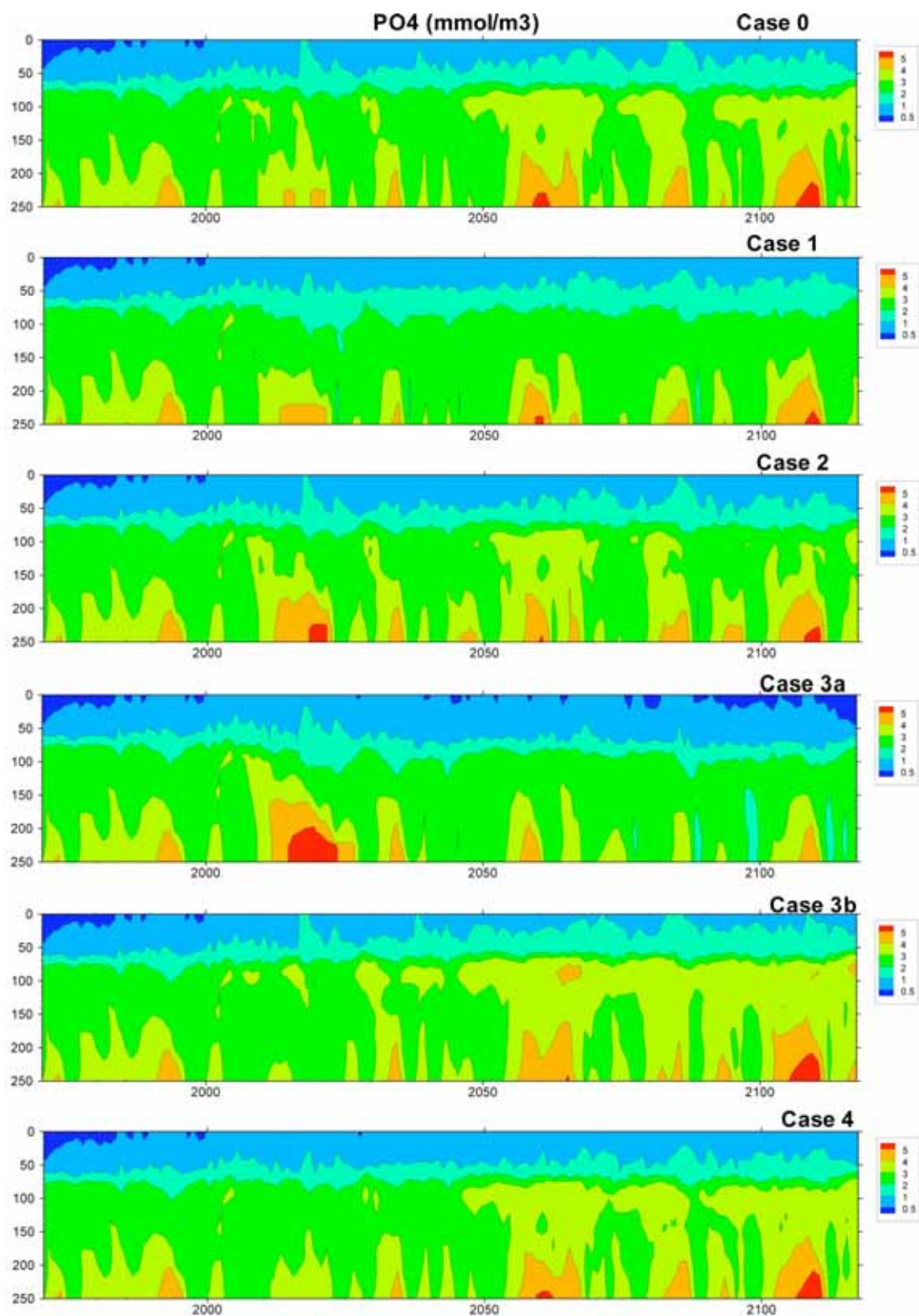


Figure 3.2.6: Temporal development of phosphate in Baltic proper from the BALTSEM simulations.

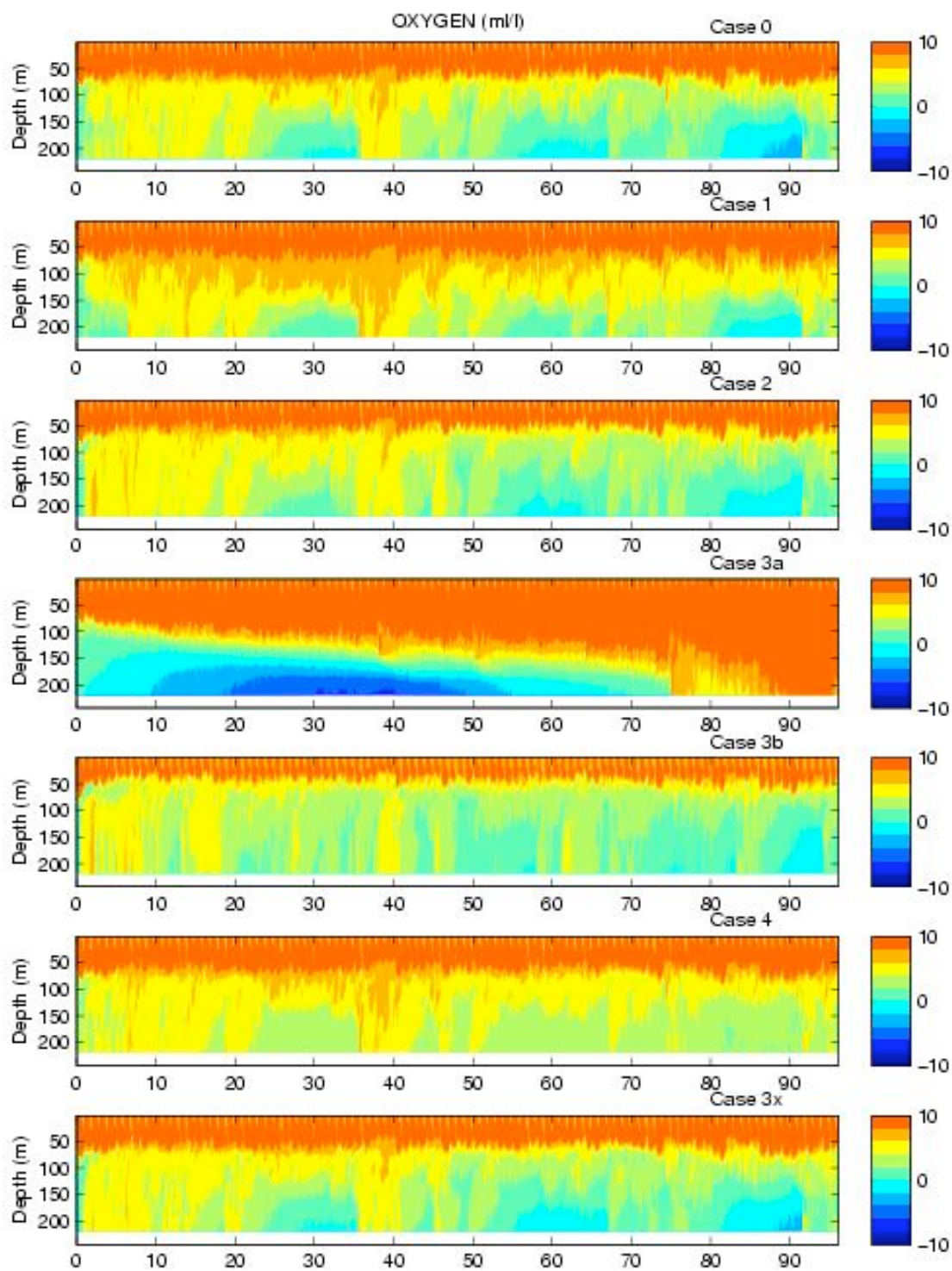


Figure 3.2.7: Temporal development of oxygen in the Eastern Gotland Basin from the RCO-SCOBI simulations.

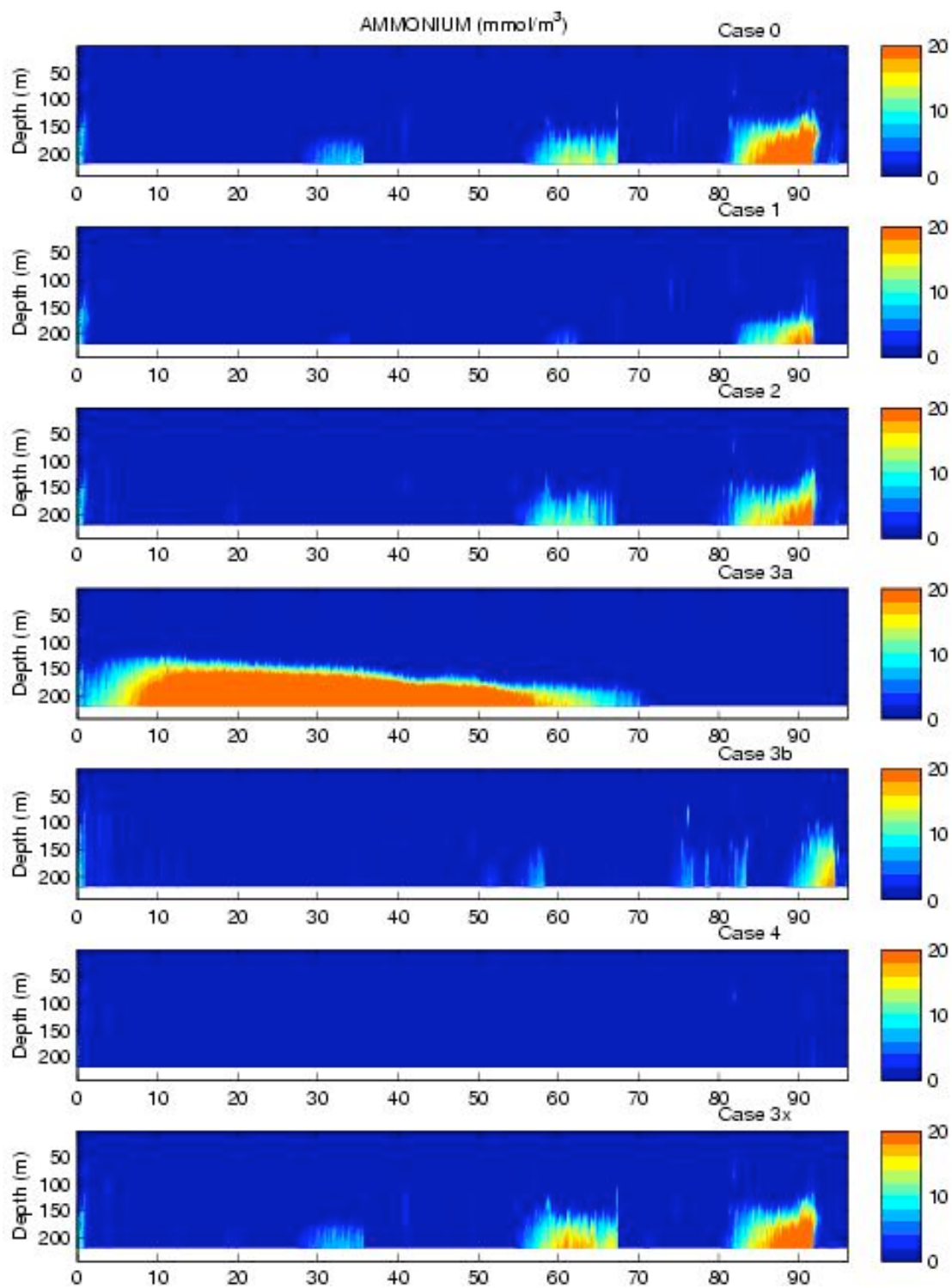


Figure 3.2.8: Temporal development of ammonium in the Eastern Gotland Basin from the RCO-SCOBI simulations.

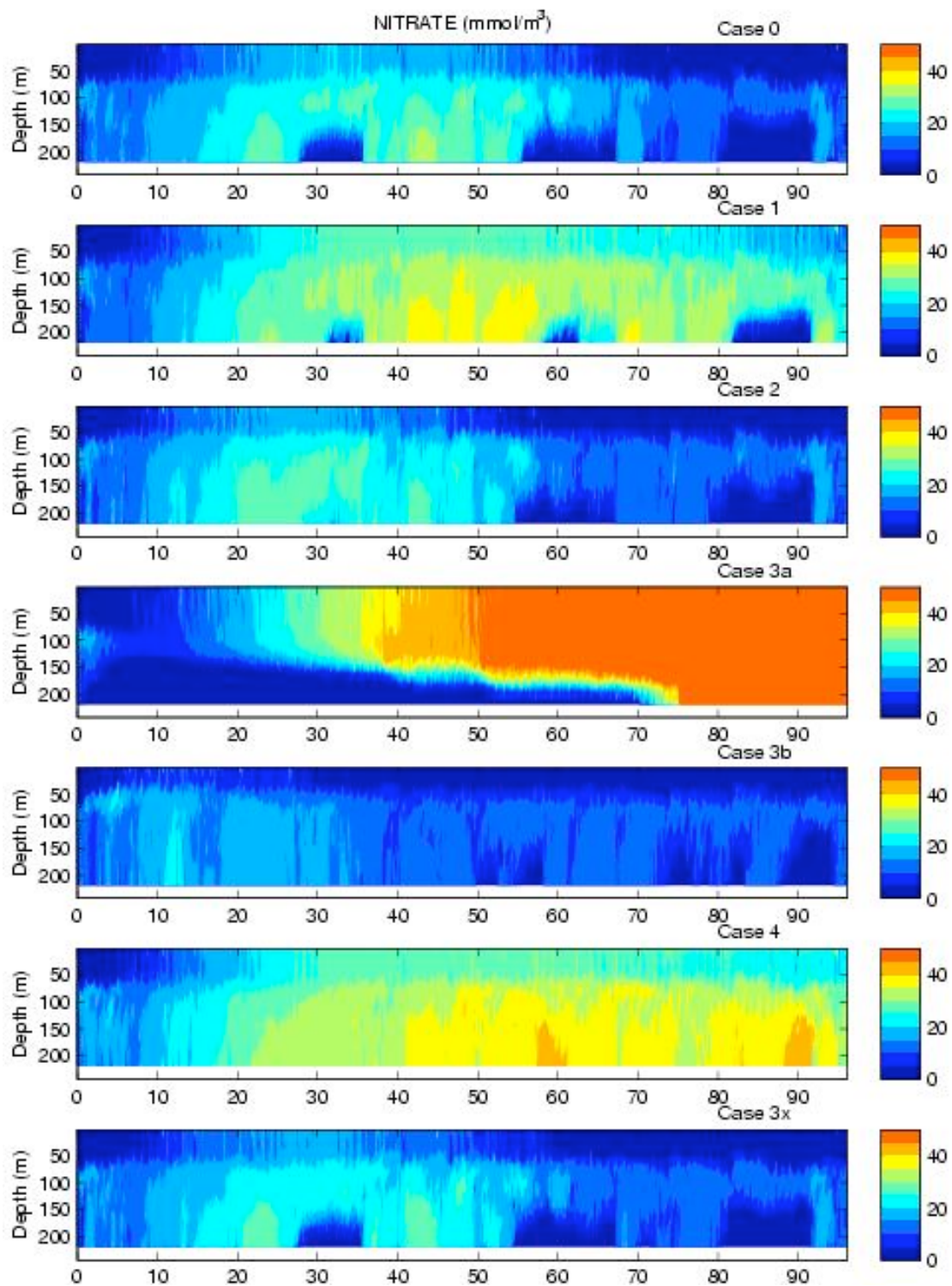


Figure 3.2.9: Temporal development of nitrate in eastern Gotland basin from the RCO-SCOBI simulations.

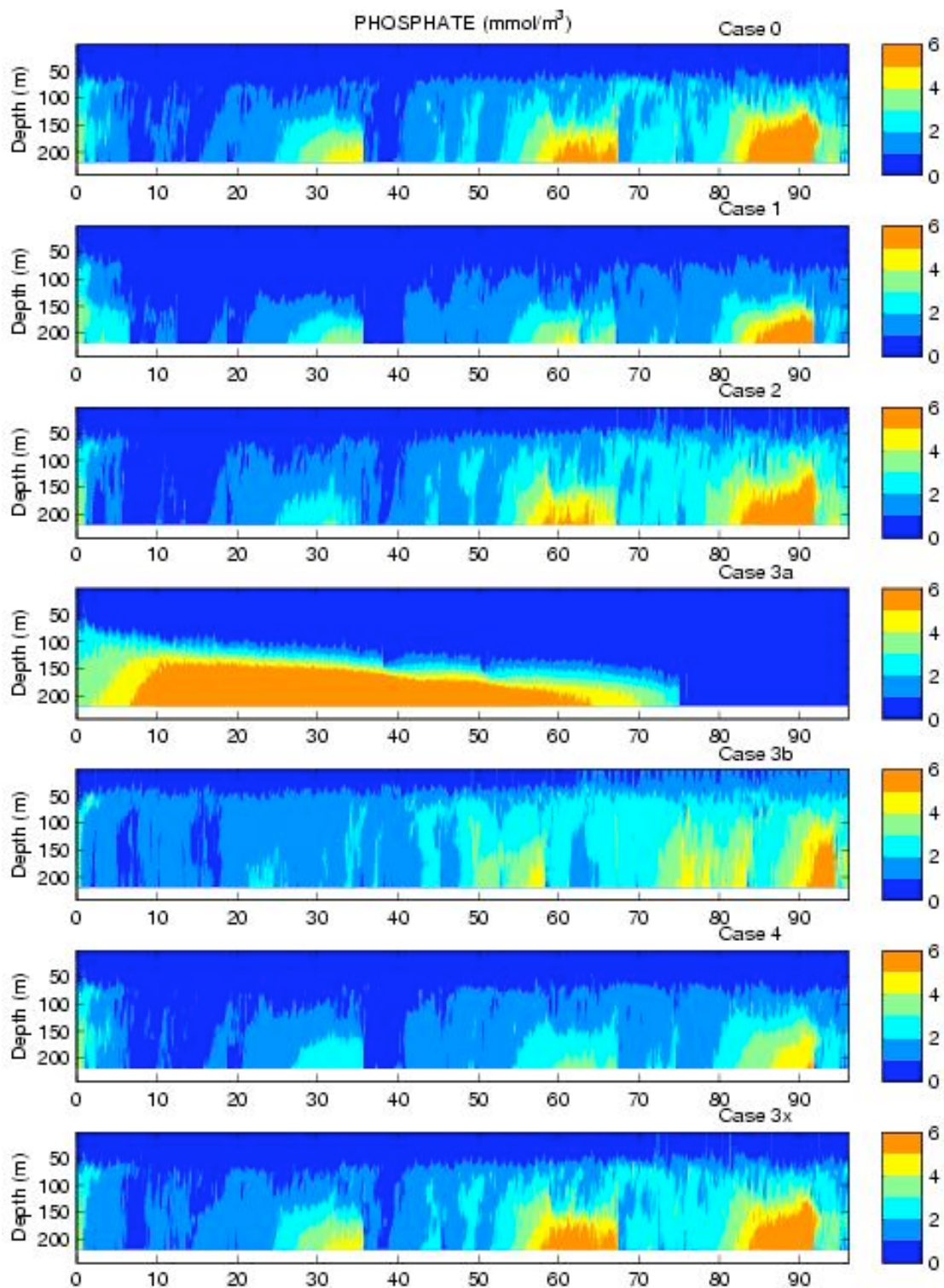


Figure 3.2.10: Temporal development of phosphate in eastern Gotland basin from the RCO-SCOB simulations.

### **3.3 Horizontal variations**

In this section we illustrate the horizontal variations for selected model results. The surface salinity distributions are drawn in Figure 3.3.1 and 3.3.2 for RCO-SCOB1 and BALTSEM results, respectively.

Comparing these, one may see one reason for the differing results in Case 2. The salt lock induces more unidirectional flow towards the Baltic through the Great Belt and from the Baltic through the Öresund. In RCO-SCOB1, the fresh outflow and the salty inflows may be spatially separated in the southern Kattegat, while in BALTSEM they are mixed in the southern Kattegat box. In RCO-SCOB1 the mixing between these water masses is smaller resulting in an inflow of more saline water in the Baltic while the fresher outflow through Öresund to a large degree is transported further into the North Sea.

Horizontal gradients within the Baltic Sea change more in RCO-SCOB1 results for Cases 3a and 3b, than in BALTSEM results. This is probably mainly due to the larger salinity changes in general in RCO-SCOB1 results, and for large deviations from present condition one would expect less linear response. In Case 3a the salinity is quite low which does not allow for strong gradients and in Case 3b the salinity is rather high which will make gradients quite strong in the vicinity of the large river outlets.

From Figures 3.3.3 and 3.3.4 showing bottom salinities it is clear that halocline ventilation (Case 1) does not affect deep water conditions outside the deepest basins of the Baltic proper.

It is clear in both models results (Figures 3.3.5 and 3.3.6) that bottom oxygen in Gulf of Finland is quite sensitive to the changes between different cases. This is due to the fact that the depths are located close to depth of the strongest oxygen gradients.

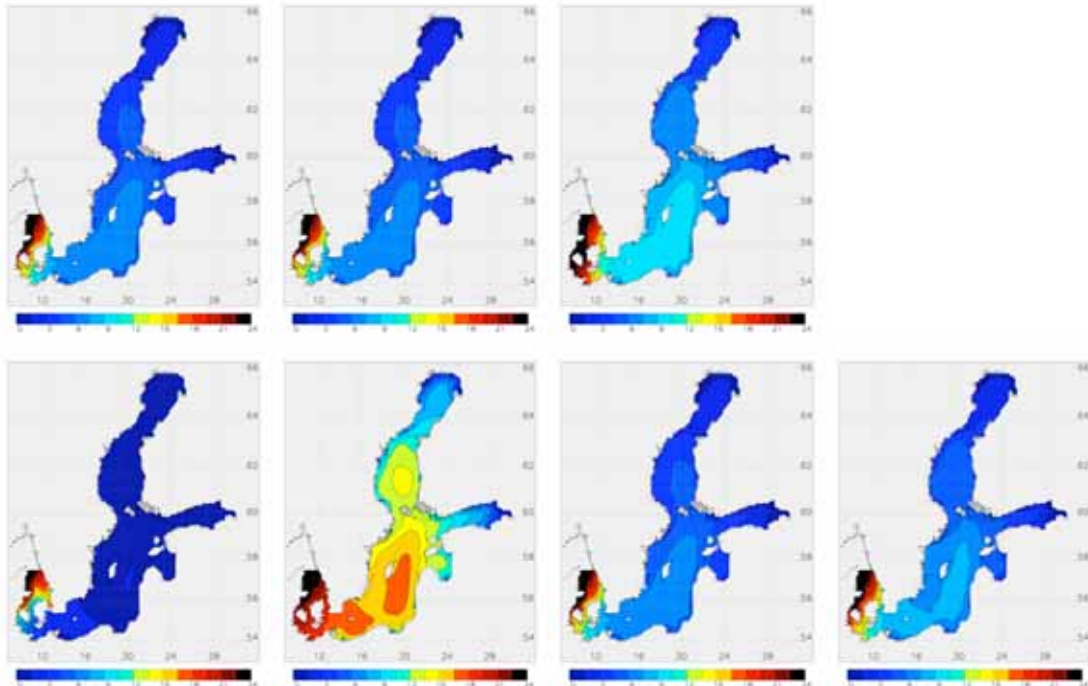


Figure 3.3.1: Average surface salinity distributions from the RCO-SCOBI simulations. From left, the upper row of panels shows the cases 0, 1 and 2 and the lower row shows the cases 3a, 3b, 4 and 3x.

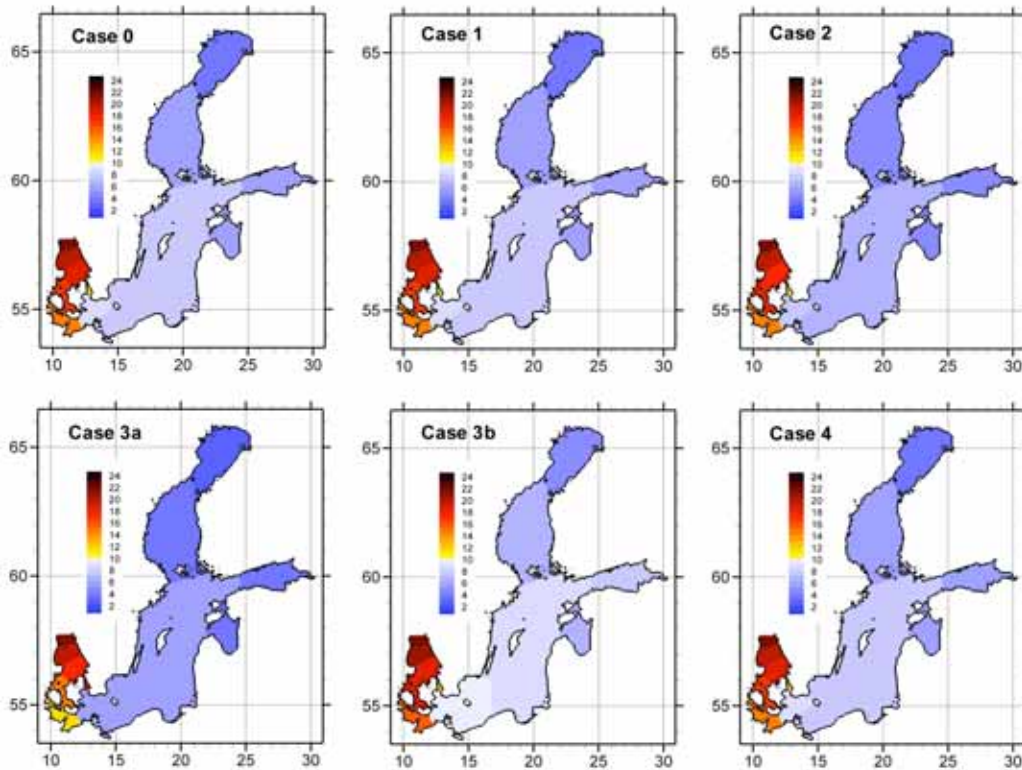


Figure 3.3.2: Average surface salinity distribution from BALTSEM simulations.

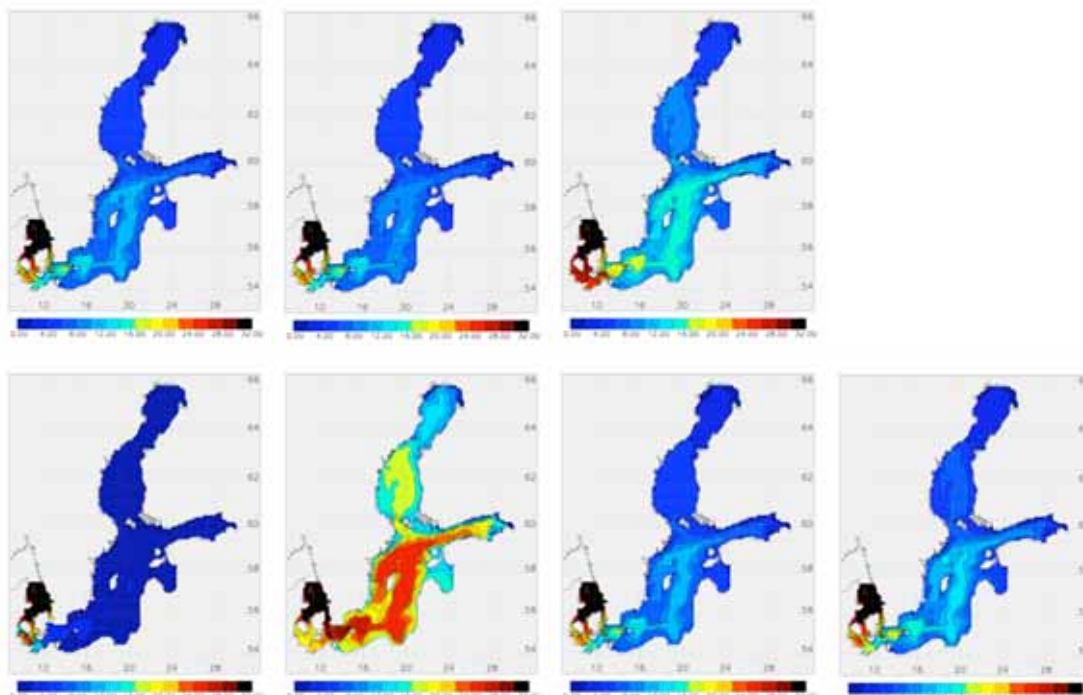


Figure 3.3.3: Average bottom salinity distributions from the RCO-SCOBI simulations. From left, the upper row of panels shows the cases 0, 1 and 2 and the lower row shows the cases 3a, 3b, 4 and 3x.

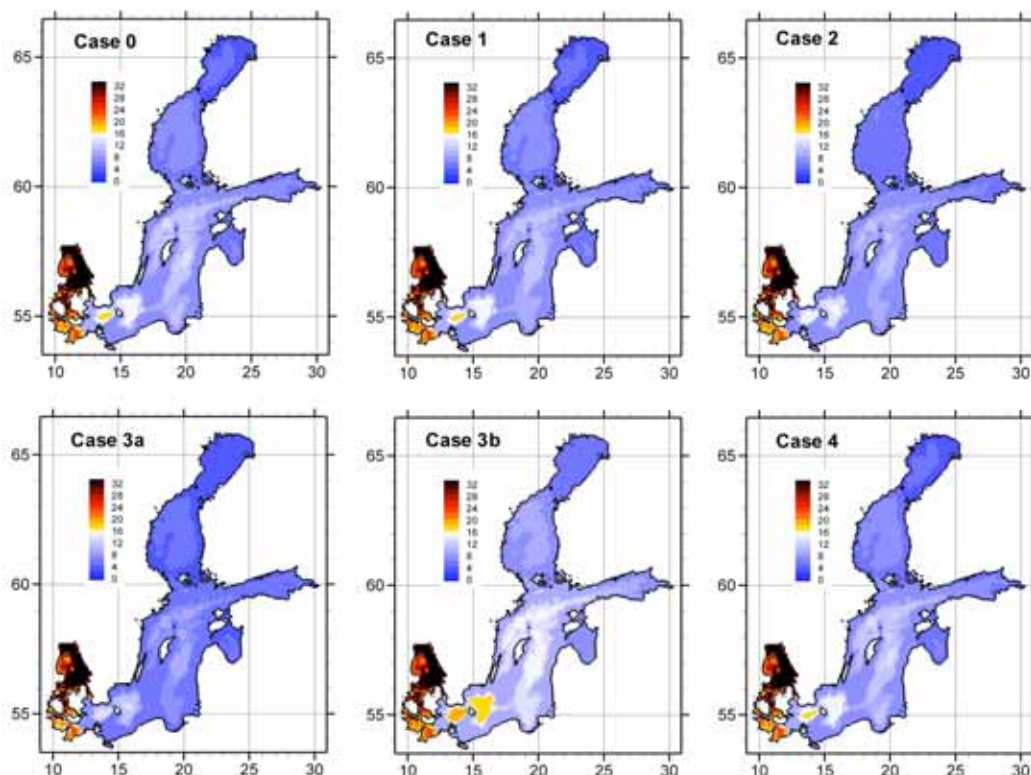


Figure 3.3.4: Bottom salinity distributions from the BALTSEM simulations. The vertical salinity profile for each basin is projected on the topographic map of the Baltic Sea.

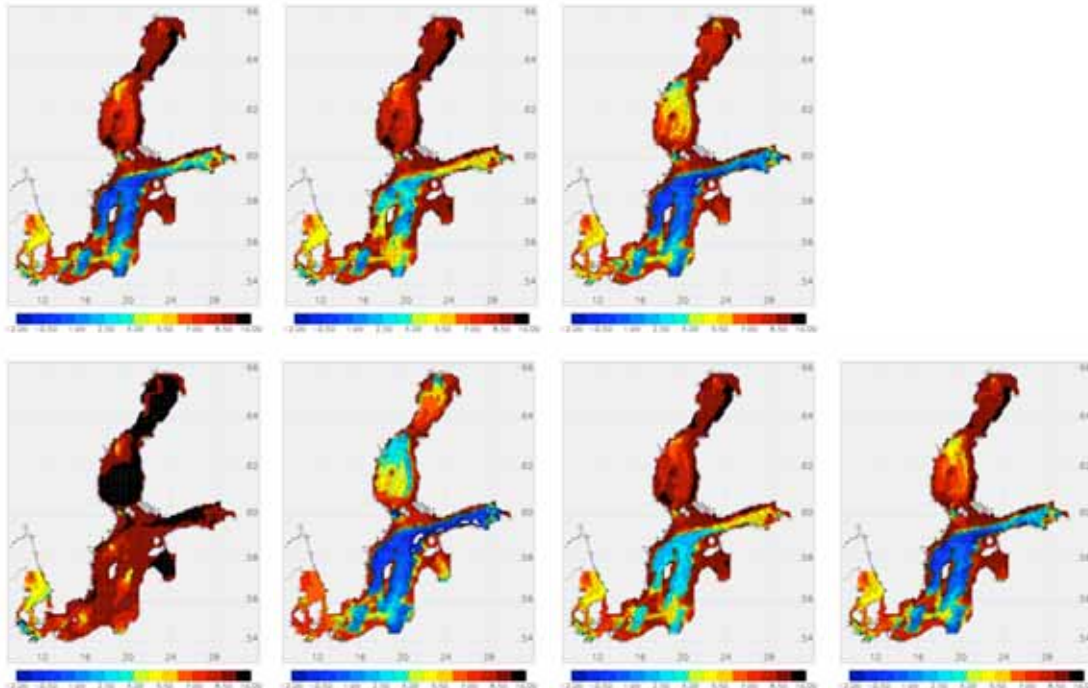


Figure 3.3.5 Average bottom oxygen concentrations from the RCO-SCOBI simulations. From left, the upper row of panels shows the cases 0, 1 and 2 and the lower row shows the cases 3a, 3b, 4 and 3x.

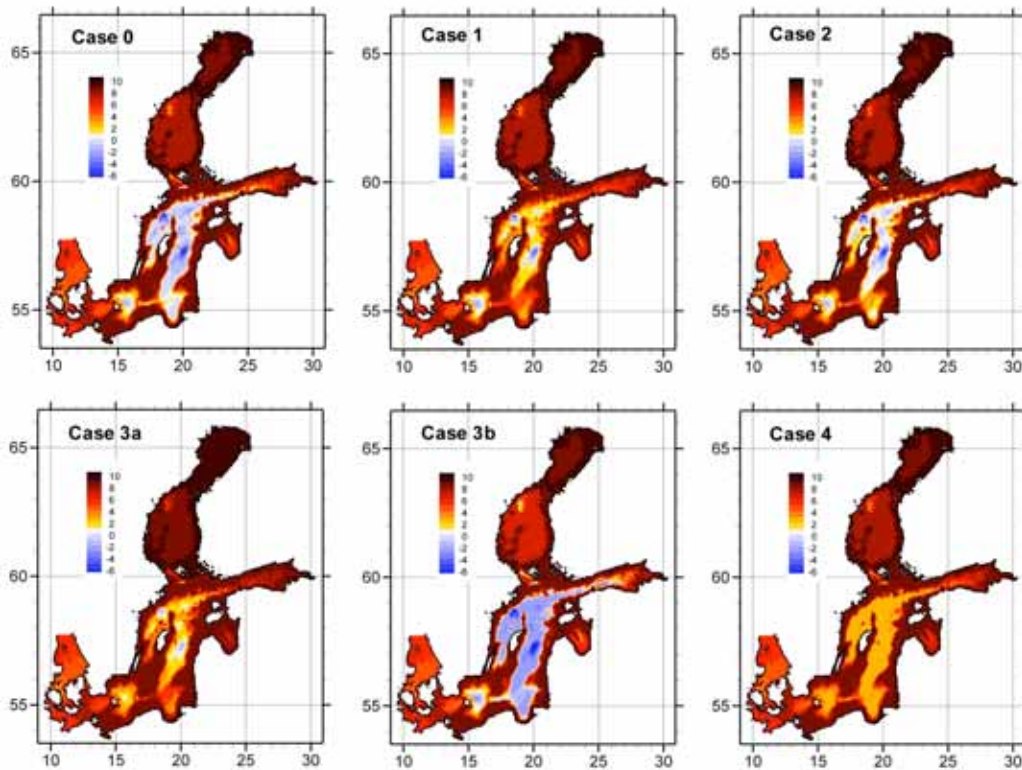


Figure 3.3.6: Bottom oxygen concentrations from the BALTSEM simulations. The vertical oxygen profile for each basin is projected on the topographic map of the Baltic Sea.

### 3.4 Nutrient budgets

The average total phosphorus content has been calculated from the model results (Figure 3.4.1). BALTSEM has in all cases more phosphate than RCO-SCOBI, but as indicated above in the average profiles, RCO-SCOBI responds stronger to the changes between cases.

Overall nutrient budgets have been computed as average of the last 30 years of the simulations with BALTSEM (Tables 3.4.1 and 3.4.2). We present the nutrient budget for the initial 1970 – 2006 simulation as further reference. The column with load and exchange includes the nutrient loads plus the net import through the model boundary, in this case between Arkona and Bornholm basins. The loads are the same for all cases, but differ slightly between cases and the base simulation. Since the boundary concentrations are fixed in Arkona, the net exchange depends only on concentrations in the Bornholm basin and the volume flows. The only significant changes in exchange occur for phosphorus in Case 3a and 3b. Variations in nitrogen fixation are compensated primarily by changes in denitrification and not by burial or exchange. In all cases burial of nitrogen comprise of about 10% and denitrification 90% of the nitrogen losses

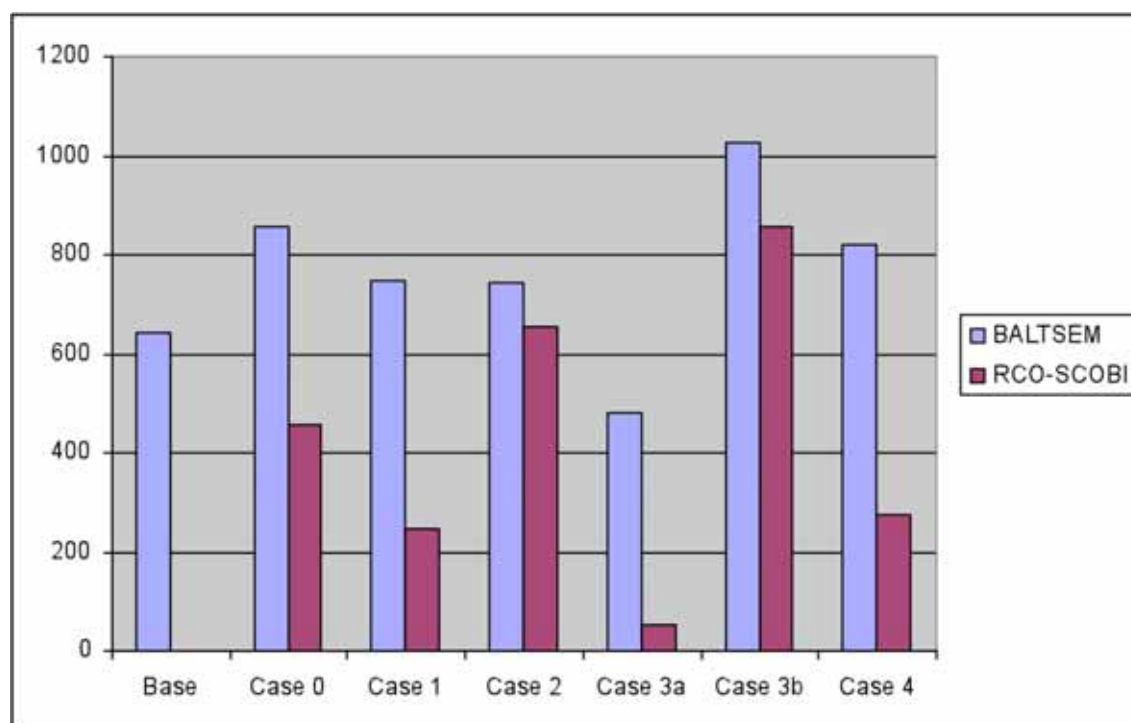


Figure 3.4.1: The pelagic phosphate content (kTons) from the last 30 years of the simulations.

Nitrogen (kT/yr)	Load & Exchange	Nitrogen fixation	Denitrification	Burial	Uptake by primary production
Base (1970-06)	654	501	998	103	8746
Case 0	626	880	1371	137	10400
Case 1	624	738	1247	139	10056
Case 2	629	699	1222	126	9292
Case 3a	638	271	838	97	5407
Case 3b	624	1072	1536	150	11646
Case 4	624	720	1221	138	9941

Table 3.4.1: Nitrogen budget for the Baltic Sea inside the Arkona – Bornholm basin boundary calculated with BALTSEM. The load & exchange column includes both external load and net exchange through the open boundary.

Phosphate (kT/yr)	Load & exchange	Burial	Uptake by primary production
Base (1970-06)	36	22	1249
Case 0	31	28	1486
Case 1	33	31	1437
Case 2	33	30	1327
Case 3a	40	36	772
Case 3b	28	26	1664
Case 4	33	31	1420

Table 3.4.2: Phosphorus budget for the Baltic Sea inside the Arkona – Bornholm basin boundary calculated with BALTSEM. The load & exchange column includes both external load and net exchange through the open boundary. Note the large storage change in the Base simulation manifested by a difference between supply and burial.

### 3.5 Change in hypoxic area and cod spawning volume

The average hypoxic ( $\leq 2$  ml/l) and anoxic ( $\leq 0$ ) areas have been computed for the last 30 years of the simulations. The results are shown in Figures 3.5.1 and 3.5.2. Cases 1, 3a and 4 show decreased hypoxic areas. BALTSEM also show decreased hypoxia for case 2. Except for Case 2, the models respond similarly as to the variations in extension of hypoxic areas. Also the spatial distributions of frequency of hypoxia are quite similar (Figures 3.5.3 – 3.5.4). The variations in cod spawning volume (Figure 3.5.5 and 3.5.6) are caused by variations in the salinity of the Baltic Sea and only very slightly influenced by decrease in hypoxic areas. Due to a programming error, cod spawning volumes are not presented from the BALTSEM simulations.

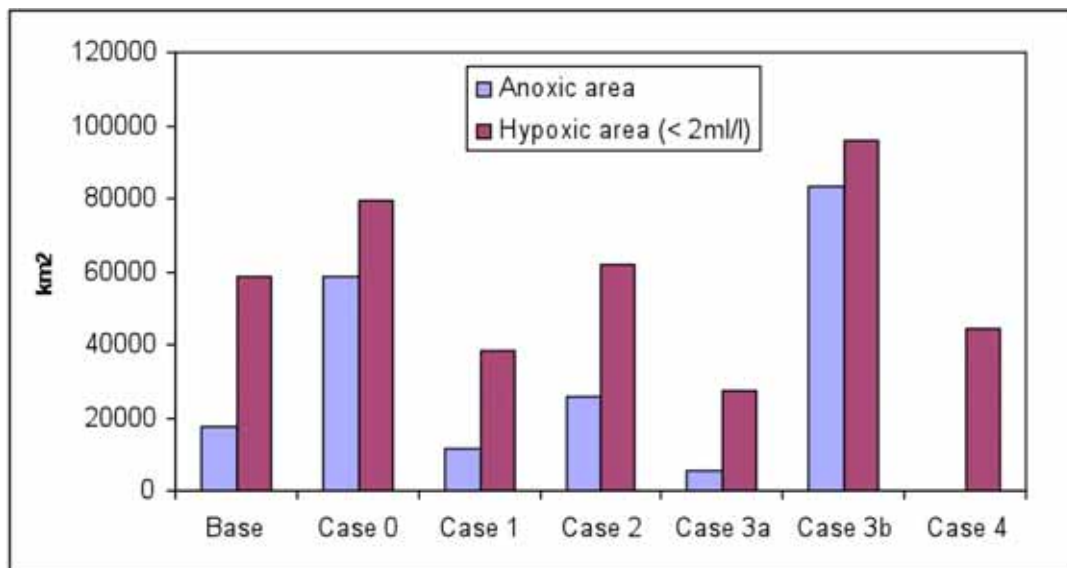


Figure 3.5.1: The average hypoxic ( $\leq 2$  ml/l) and anoxic ( $\leq 0$ ) areas from the base period and from the last 30 years of the simulations with BALTSEM.

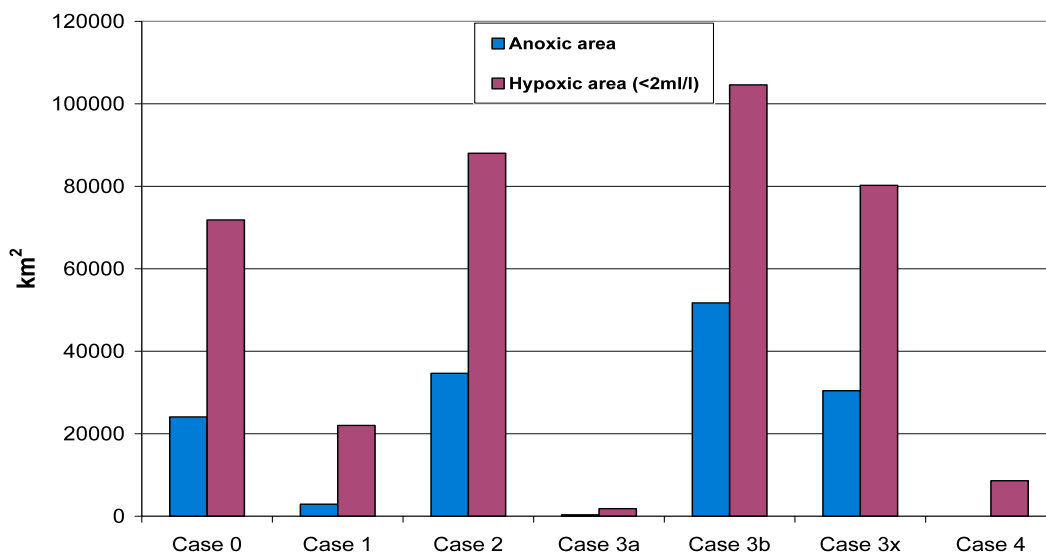


Figure 3.5.2 Average hypoxic ( $\leq 2$  ml/l) bottom area for the last 30 years of the simulations with RCO-SCOBI.

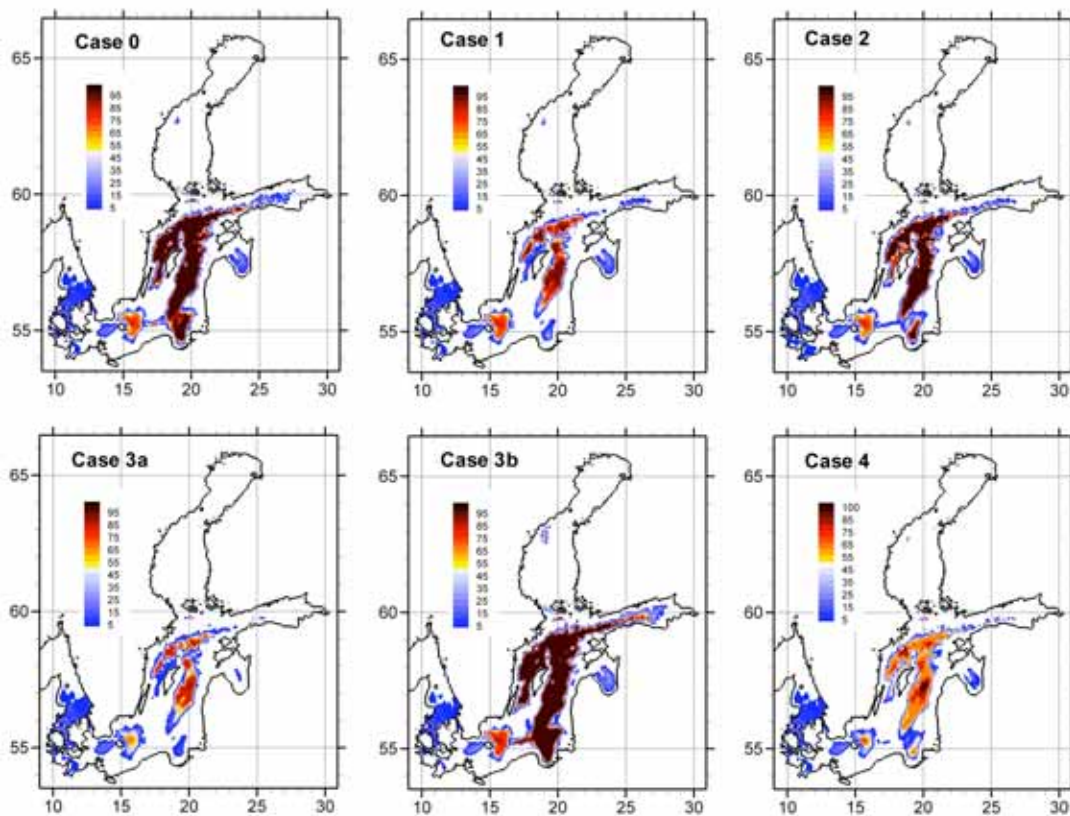


Figure 3.5.3: Spatial distribution of the percentage of time with hypoxic bottoms in BALTSEM.

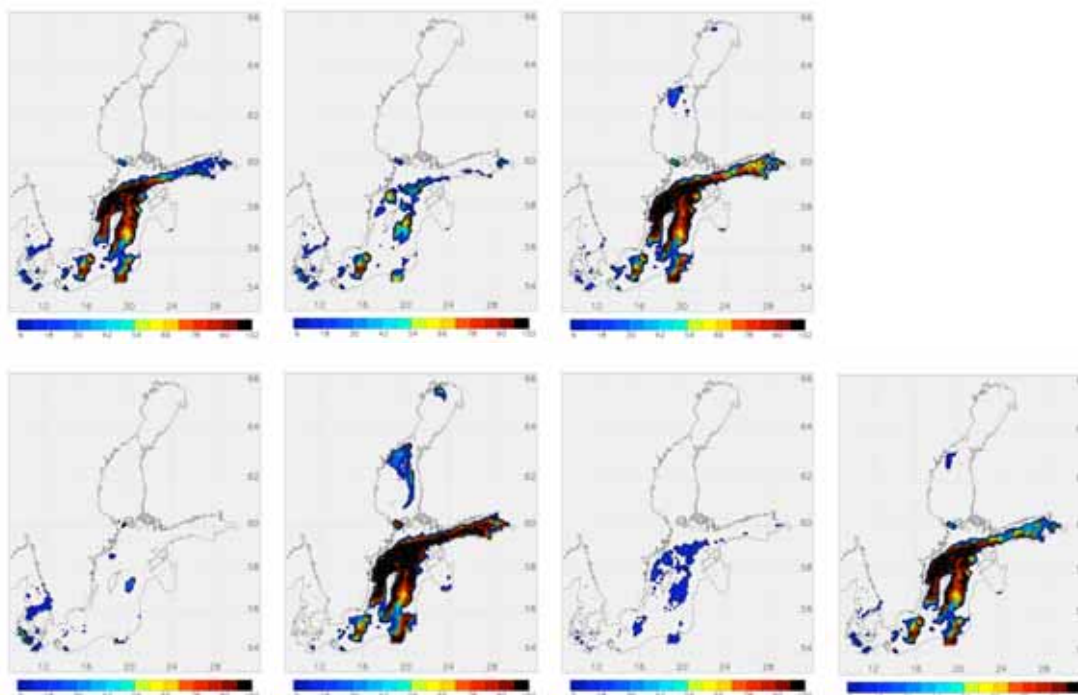


Figure 3.5.4: Spatial distribution of the occurrence of hypoxic bottoms in percent of time in RCO-SCOBI. From left, the upper row of panels shows the cases 0, 1 and 2 and the lower row shows the cases 3a, 3b, 4 and 3x.

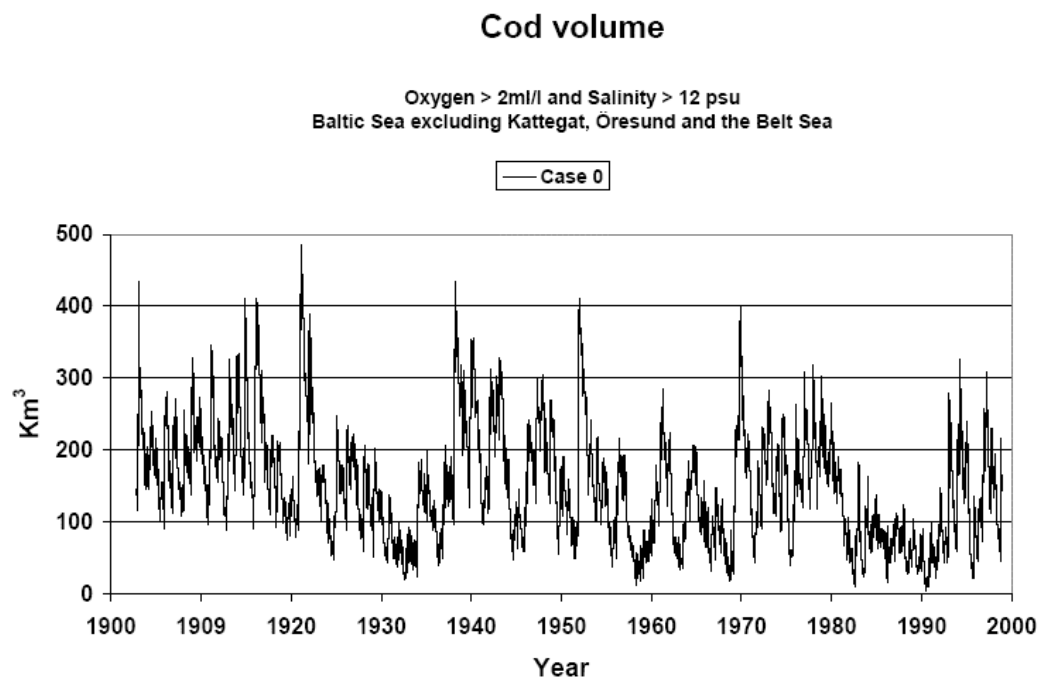


Figure 3.5.5 Cod spawning volume variations in the standard case (Case 0) in RCO-SCOBI.

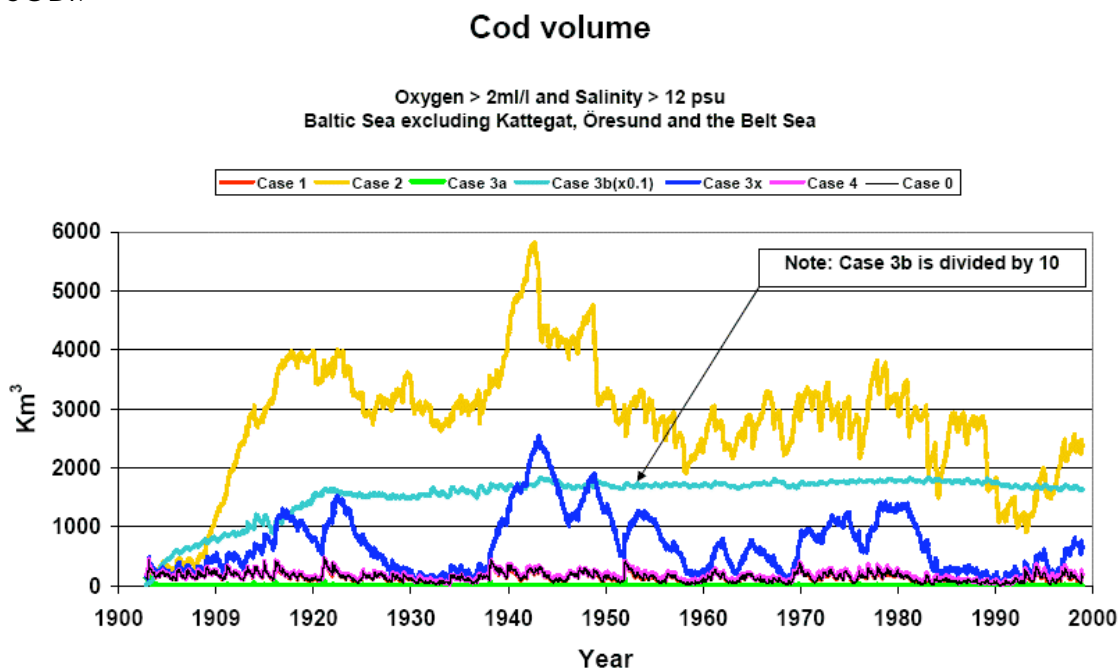


Figure 3.5.6. Cod spawning volume in all cases in RCO-SCOBI.

### 3.6 Oxygen demand (Case 4)

In case 4, we added oxygen with an artificial source in order to keep concentrations above 2 ml/l. By bookkeeping we computed the annual supply of oxygen needed (Figures 3.6.1-

3.6.2). The average was about  $2 \times 10^6$  ton/yr for BALTSEM and between 2 and  $6 \times 10^6$  ton/yr for RCO-SCOBI.

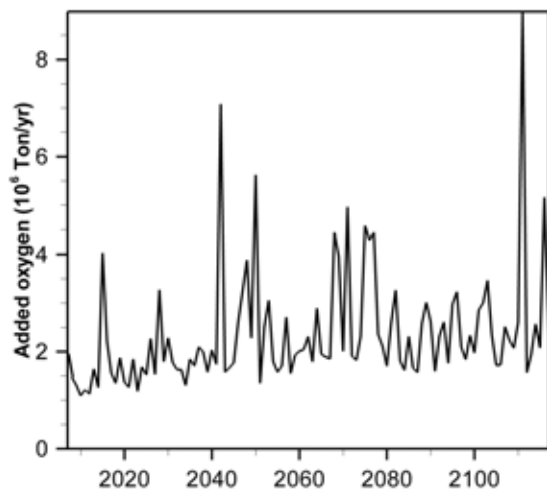


Figure 3.6.1: The amount of oxygen added each year of simulation (Case 4) calculated with BALTSEM.

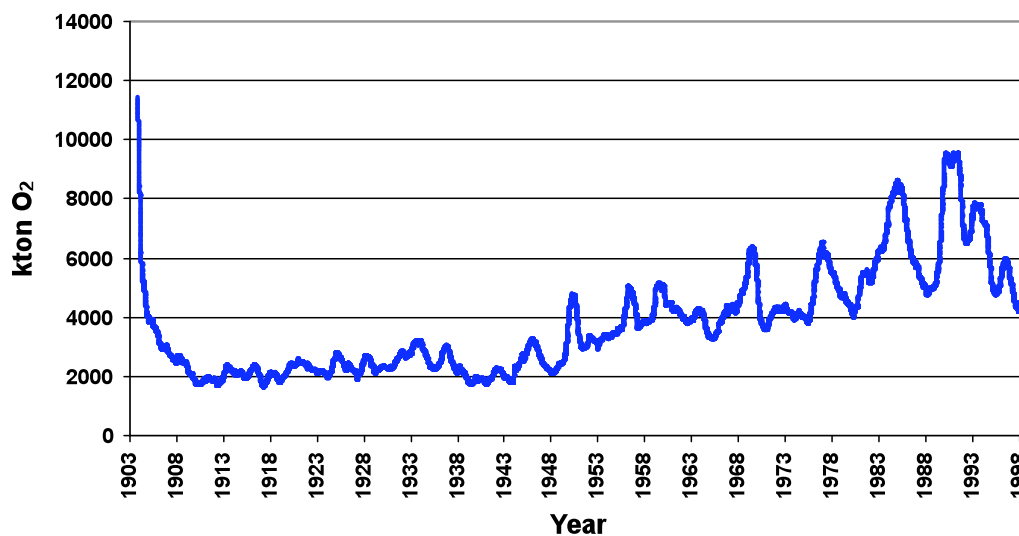


Figure 3.6.2 Supply of oxygen needed to keep oxygen concentration above 2 ml/l in RCO-SCOBI.

### 3.7 Phosphorus burial

The major long-term sink of phosphorus is permanent removal through burial in the sediments. In the models most are buried in the layers above 150m. RCO-SCOBI show an increased burial towards the surface layers while BALTSEM has a maximum around 50m depth (Figures 3.7.1 and 3.7.2).

The spatial distribution of burial from RCO-SCOBI (Figure 3.7.3) shows that significant burial fluxes occur at shallow depths in the close proximity of major river sources. Hot spots seem to be found also on slopes within the basins as well.

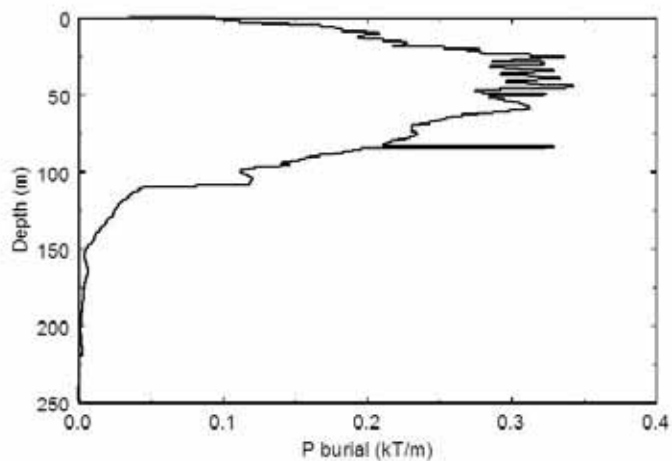


Figure 3.7.1: The vertical variation of burial of phosphorus (in  $\text{kton m}^{-1}\text{year}^{-1}$ ) in Case 0 from BALTSEM.

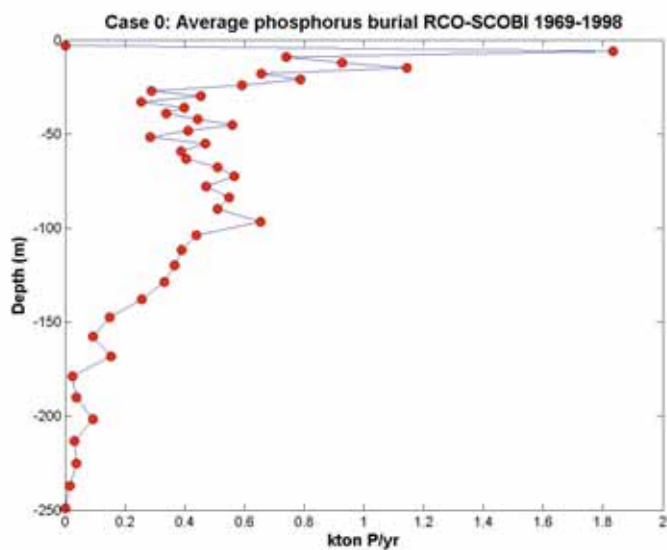


Figure 3.7.2: Phosphorus burial integrated for each depth level in Case 0 from RCO-SCOBI.

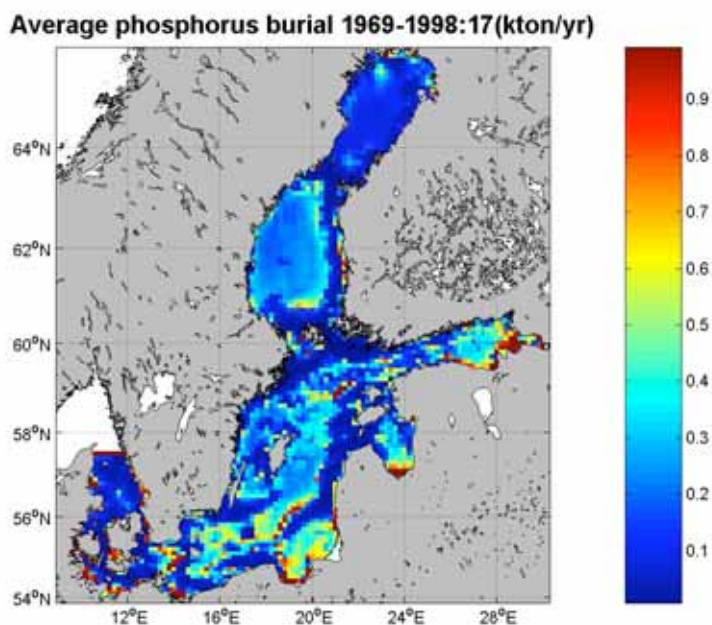


Figure 3.7.3: Spatial distribution of phosphorus burial in RCO-SCOB1.

### **3.8 Change in plankton biomass and primary production**

The changes of phytoplankton and cyanobacteria biomass in the RCO-SCOB1 model relative to Case 0 (Figure 3.8.1) are shown in Figures 3.8.2 and 3.8.3. The integrated biomass in the Baltic proper including the Gulf of Finland and the Gulf of Riga are shown in Figure 3.8.4. In Cases 1, 3a and 4 the phytoplankton biomasses generally decrease south of the Bothnian Bay. The cyanobacteria biomass shows a similar decrease in the southern Baltic Sea. Case 2 show a general increase of total phytoplankton biomass and the largest increase of cyanobacteria biomass. In Case 3b the phytoplankton biomass increases along the coasts and in the northern Baltic, but decreases in the western and central Baltic proper. The cyanobacteria biomass decrease in southern Baltic proper and increase in the Gulf of Finland and the northern Baltic Sea.

The corresponding results from BALTSEM are presented in Figures 3.8.5 to 3.8.7. The surface phytoplankton concentrations decrease for all cases except Case 3b. The largest decrease is in Case 3a, as expected from results above. Phytoplankton concentration decreases are especially large in Gulf of Riga in cases 2, 3a and 4. However, this is also the area with highest concentration. The overall pattern is also evident from cyanobacteria concentrations.

The integrated average biomasses for total phytoplankton and for the separate phytoplankton groups (Figure 3.8.7) show the same differences between cases as the

spatial surface concentrations. The largest reduction in all biomasses is in Case 3a. An interesting result is that dinoflagellate biomass was higher in the less eutrophic Base run than in Case 0. Further, cyanobacteria biomass is somewhat lower in Case 4 compared to Case 0, but diatom and dinoflagellate biomasses are slightly higher.

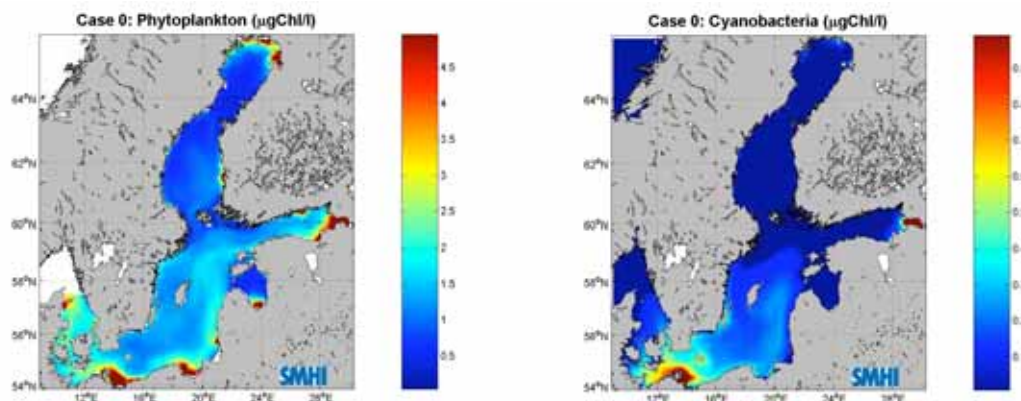


Figure 3.8.1 Average (June – September) phytoplankton and cyanobacteria biomass in the upper 10 m from RCO-SCOBI.

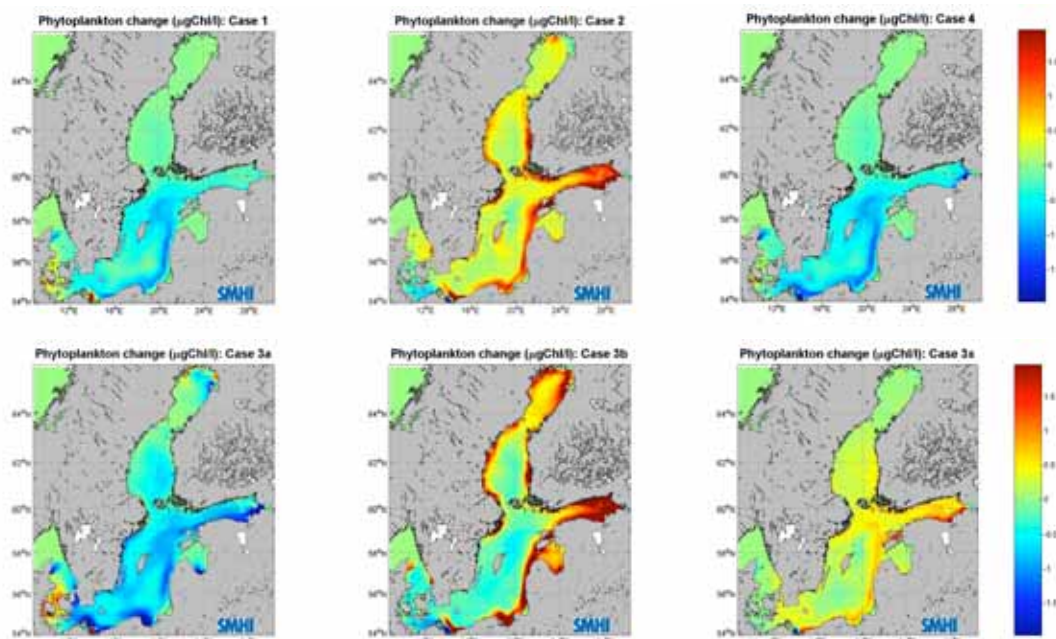


Figure 3.8.2 Deviation from phytoplankton biomass in the Case 0 simulation presented in Figure 3.8.1.

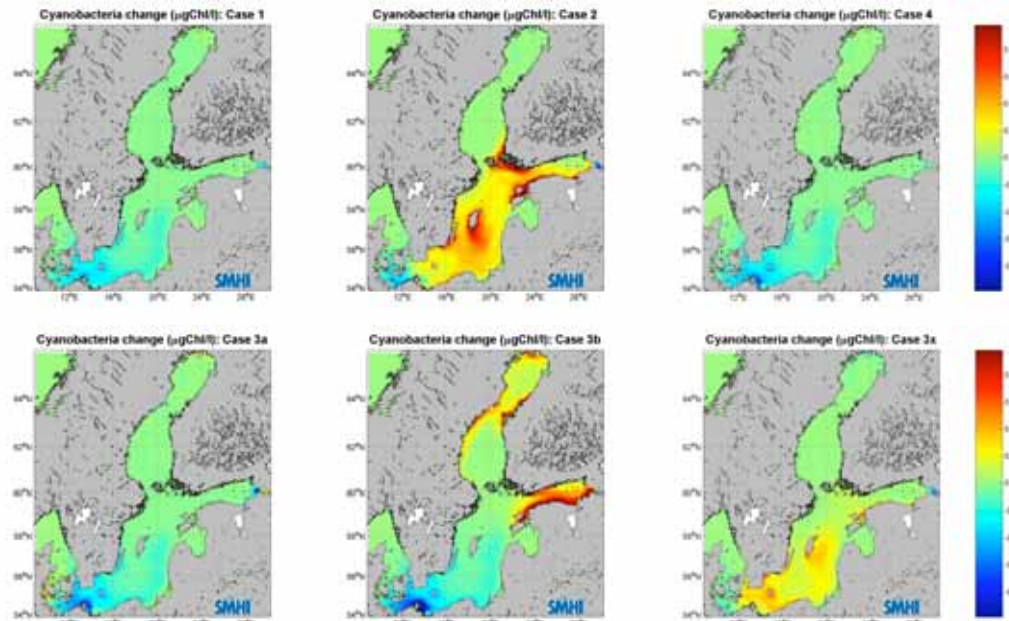


Figure 3.8.3: Deviation from cyanobacteria biomass in the Case 0 simulation presented in Figure 3.8.1.

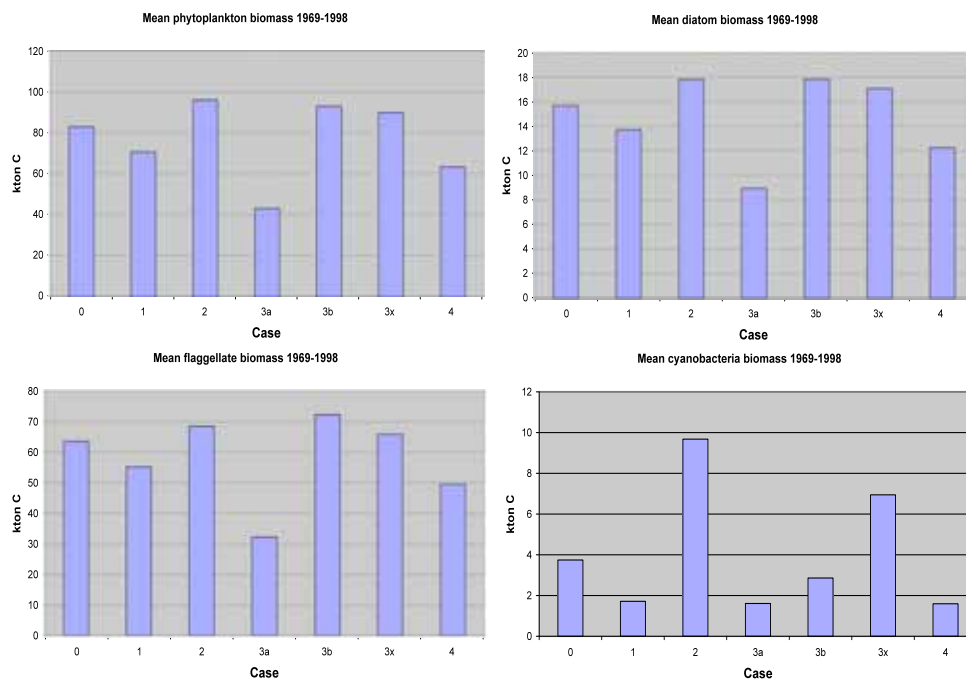


Figure 3.8.4. Integrated (0 - 40 m) annual averaged biomass of total phytoplankton and the different phytoplankton groups in the Baltic proper including the Gulf of Finland and the Gulf of Riga. Results from RCO-SCOBI.

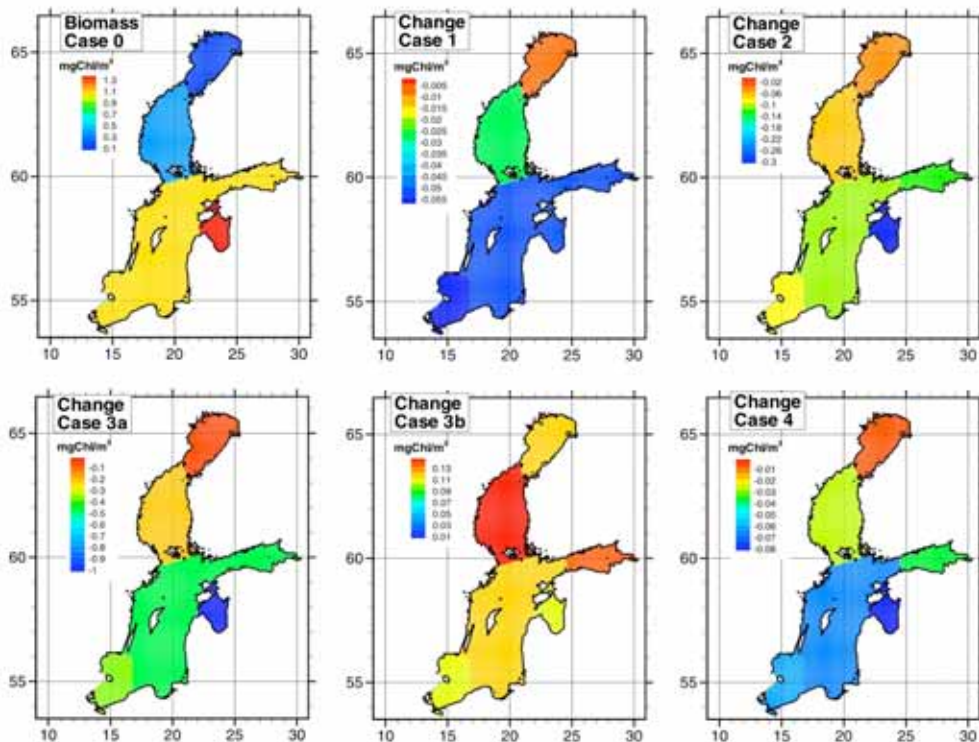


Figure 3.8.5: Average (annual) phytoplankton concentration in the surface mixed layer from BALTSEM in Case 0 (top left panel) and difference between the different cases and Case 0. Note that the scale is different in each panel.

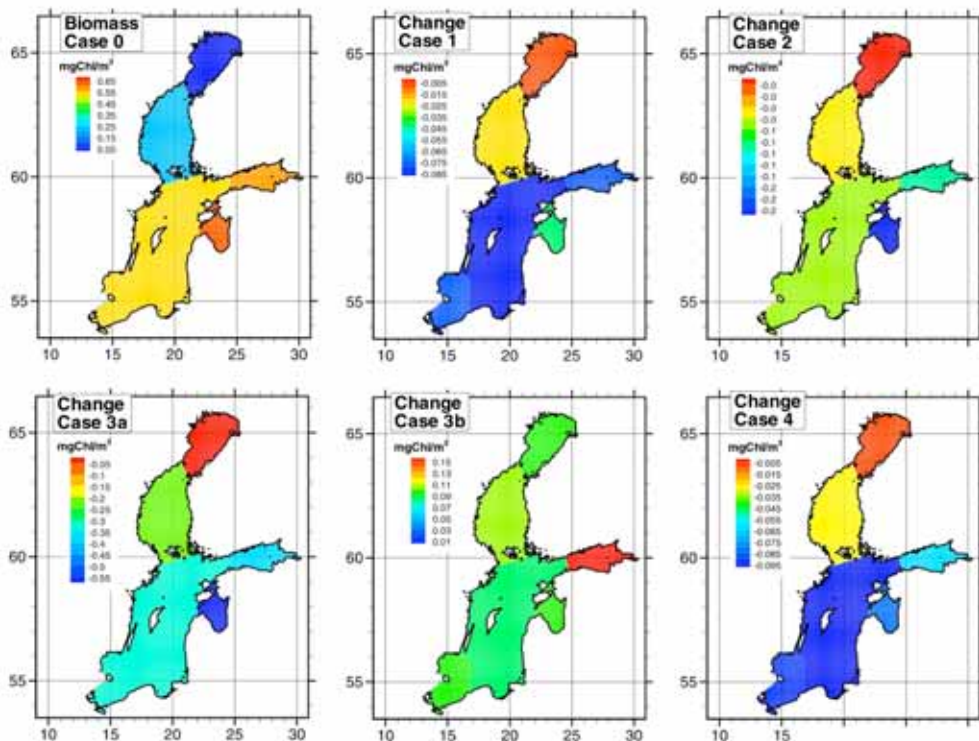


Figure 3.8.6: Average (annual) cyanobacteria concentration in the surface mixed layer from BALTSEM Case 0 simulation (upper left panel) and difference in concentrations between each case and Case 0. Note that the scale is different in each panel.

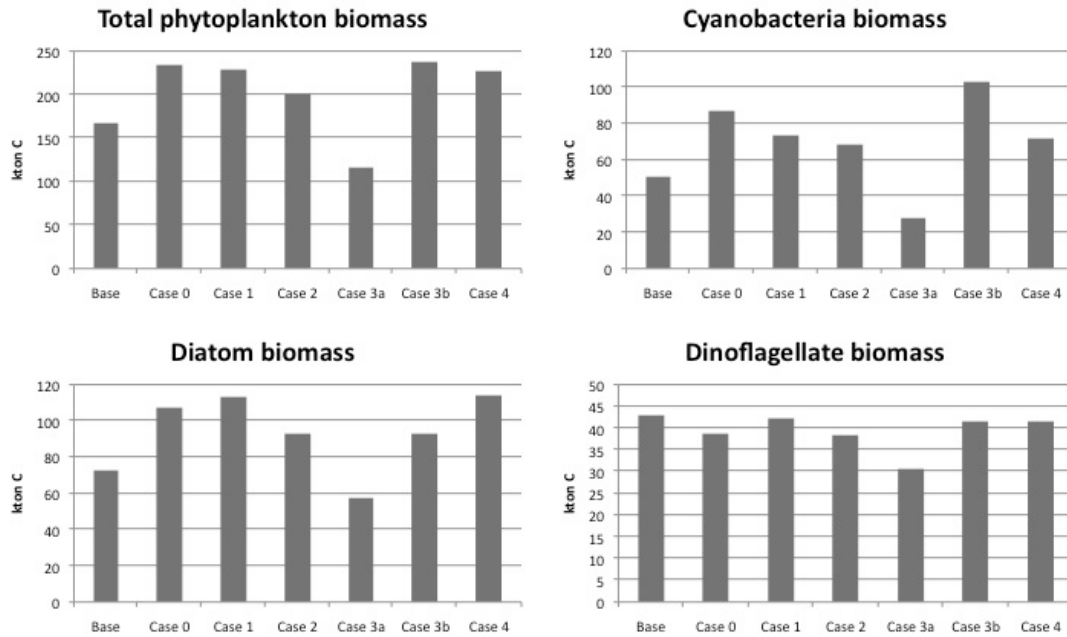


Figure 3.8.7: Integrated (whole volume) annual averaged biomasses from Baltic proper, including Gulfs of Finland and Riga, and Gulf of Bothnia. Results from BALTSEM.

#### 4 Discussion

Apart from different formulations in the models are differences in the implementation a major cause for different model sensitivities. The results depend on the initial conditions of the models since the state of the sea is changing during the studied period. The time scales of nutrient cycling in the model Baltic Sea (excl. Kattegat) are mainly set by the combined residence time in water and in sediments, and are therefore quite long (many decades). It was decided early that the models should be used "as is" for these simulations and therefore the models use different initial conditions and different physical forcing for the studied period, which therefore results in quantitatively different model responses.

The RCO-SCOB1 was initialized by spin-up during more than a century while BALTSEM was initialized by best "guesstimates" of water and sediment concentrations. The models have then been calibrated using these initial conditions. All consequences of this are still not explored. One obvious consequence was that BALTSEM forecasts an increased eutrophication if present loads continue into the future (Case 0), while RCO-SCOB1 is in more balance. Thus, we have different preconditions in Case 0. BALTSEM is hypoxic below about 75 m depth and anoxic below about 90 m depth at the eastern Gotland Deep (BY15) while RCO-SCOB1 is hypoxic below about 125m. This influences e.g. the vertical distribution of nutrients between the sediments of the two models. This in turn influences the different sensitivity of the biogeochemical models.

The RCO-SCOB1 3D model may have bottoms covered with low oxygen also in shallower areas due to regional differences in biological oxygen consumption and physical circulation. A horizontally averaged model like BALTSEM has the same oxygen concentrations at the bottoms of the rim of the sub-basins as in the offshore deep water. A similar discussion is also true for the larger ranges of horizontal salinity distribution in the RCO-SCOB1 model compared to BALTSEM. Both these issues may influence the different sensitivity of the biogeochemical models.

Occasions with resuspension of sediments may transport phosphorus that is bound in shallow and well-oxidized sediments to deeper anoxic and hypoxic layers where the phosphorus may become released to the water again. The mechanisms of resuspension differ between the models, e.g. RCO-SCOB1 has lower resuspension than BALTSEM in shallow waters. This also influences the different sensitivity of the biogeochemical models.

#### **4.1 Discussion of consequences of each engineering solution:**

##### *4.1.1 The magnitude of the disturbance on physical circulation of the Baltic proper*

RCO-SCOB1 is more sensitive to closing (Case 3a) or dredging (Case 3b) the Öresund than BALTSEM. As the horizontal grid resolution of 6 nautical miles is rather coarse in comparison with the dimensions of the straits in the Baltic entrance, a proper representation of the topography in any three-dimensional circulation model is problematic. Although it is possible to adjust the flow ratio in present climate (Case 0) such that both the total volume and salt flows into the Baltic are realistically simulated, any changes of the cross section would very likely not have the correct sensitivity on the simulated salt flows. However, as the impact from dredging or closing the Öresund on the stratification and internal circulation is similar in both models (BALTSEM and RCO-SCOB1), and basically only differ in magnitude, the conclusion that any realistic engineering method affecting the exchange through the Danish straits does not improve the oxygen conditions during the coming decades is robust.

The salt lock case (Case 2) is more difficult to interpret. Two competing effects (increased sea levels in the Baltic hamper the inflow versus increased salt flow due to opening/closing of the salt lock) determine the impact of the simulated salt lock. Details of the implementation differ in the models as outlined above. To ensure the robustness of the results the simulation with RCO-SCOB1 was repeated with an increased horizontal grid resolution of 2 nautical miles. It was earlier shown that this resolution is sufficient to

simulate both the volume and salt flows through Öresund in close agreement with observations (Meier et al., 2003). In RCO the salt lock induces an additional cyclonic circulation in the entrance area (inflow through the Great Belt and outflow through the Öresund) causing a net salt flow into the Baltic. In case of outflow in the Great Belt the reduced flow capacity by the salt lock is compensated by outflow through the Öresund. The changes of the mean sea level in the experiment with salt lock compared to the reference case are relatively complex. Despite a local sea level jump in the Great Belt at the location of the salt lock a general sea level difference increase between Kattegat and the western Baltic is not observed, in contrast to BALTSEM results. Further investigations to illuminate the processes involved are necessary.

Although in Case 2 we do not obtain similar effects on exchange with the two models, our conclusions concerning the impact on the nutrient cycles and hypoxia are not affected. The prime reason is that in neither of the models does the salt lock significantly alter the frequency or duration of stagnation in the Baltic, it only modulate the amplitude of exchange. Therefore, the salt lock results resemble cases 3a and 3b. Even in case of a freshening as simulated with BALTSEM the transitional stagnation period prevents a reduction of hypoxic bottom areas.

#### *4.1.2 The change in hypoxia*

Case 1, 3a and 4 show decreased hypoxic areas. BALTSEM also show decreased hypoxia for case 2. Except for case 4, these cases correspond to situations with a lowered salinity in the deeper layers of the models. In fact, cases 2, 3a and 3b demonstrate the quite robust result that increased exchange with the North Sea cause more hypoxia as a consequence of the physical processes. Addition of oxygen with an artificial source (Case 4) requires about  $2-6 \times 10^6$  ton/yr in order to keep concentrations above 2 ml/l, which confirms the calculations by Stigebrandt and Gustafsson (2007).

#### *4.1.3 The change in plankton biomass and primary production, including cyanobacteria*

In Cases 1, 3a and 4 the phytoplankton and cyanobacteria biomasses generally decrease due to improving oxygen conditions and reduced phosphorus concentrations. However, the decrease in phytoplankton due to improved oxygen conditions only, Cases 1 and 4, is quite small in BALTSEM results, but there is a shift from cyanobacteria to diatom biomass. Case 2 which show the largest increases of phytoplankton and cyanobacteria

biomasses in RCO-SCOB1 corresponds to an increased salinity and an increase of phosphorus and slightly lowered oxygen concentrations.

In Case 3b the phytoplankton biomass increases, however slightly in BALTSEM. In the RCO-SCOB1 simulation cyanobacteria biomass decrease in southern Baltic proper and increase in the Gulf of Finland and the northern Baltic Sea. The decrease of cyanobacteria in the Baltic proper is caused by the increased salinity that inhibits the growth of cyanobacteria in the model. In BALTSEM cyanobacteria biomass increase also in southern Baltic proper because the salinity does not increase that much. There is a decrease in diatom biomass of approximately the same magnitude as the increase in cyanobacteria biomass.

#### *4.1.4 The change of cod "reproduction" volumes*

The cod spawning volume is mainly determined by the salinity of the Baltic Sea and may therefore only be increased by methods that increase the salinity of the Baltic Sea. This is however not preferable since the models show that measures causing increased salinity also cause deteriorating oxygen conditions. Increased salinity may also affect the biodiversity of the Baltic Sea

## **4.2 Major limitations and uncertainties**

Generally, there are several large sources of uncertainties common to physical-biogeochemical modeling of the Baltic Sea. One being the nutrient loads to the models, where, for example, on top of unavoidable uncertainties in determining loads and boundary concentrations different assumptions need to be made on the bioavailability of organic loads. Another source of uncertainty is the initial conditions on benthic state variables that is largely unknown and have an impact on the simulation results during a considerable time. In the present investigation, the two models have been implemented with different forcing data and different initial conditions, and that have had effects on the results.

The response of the models to the different cases generally points in the same direction, but with quite large difference in sensitivity. In general, RCO-SCOB1 reacts stronger to changes than BALTSEM, both in physical circulation to change in morphology and in biogeochemical response to, for example, changes in redox conditions. From our understanding of the models and the actual system, we believe that the range covered by the two models probably covers the response of the natural system.

Two key variables determine much of the biogeochemical response in the cases, oxygen and salinity, through the parameterizations of phosphorus retention, together with the vertical flux of particulate matter through sinking and resuspension. The biogeochemical response to oxidation (Case 4) is much stronger in RCO-SCOBI than in BALTSEM, even though Case 0 was more anoxic in BALTSEM runs. Both models are sensitive to changes in salinity, but since the salinity changes differ it is difficult to compare the strength of the sensitivities. It should be noted that phosphorus and nitrogen cycles are intimately coupled and, hence, responses in nitrogen concentrations differ as well in magnitude. Thus, the parameterizations of retention and resuspension are major sources of uncertainty in state-of-the-art Baltic Sea models.

### **4.3 Necessary future developments**

There is a need for improvement of vertical nutrient fluxes from the sediments in both models. BALTSEM has in general too high DIP concentrations in the surface and too low at depth and also RCO-SCOBI needs to be improved such that observed mean benthic profiles of nitrogen and phosphorus are reproduced. Currently a wave model and improved resuspension algorithms are being implemented into RCO-SCOBI.

BALTSEM has currently the boundary of the biogeochemical model set between Arkona and Bornholm basins. This may cause unrealistic nutrient exchange in simulations of extreme cases. The work of extending the biogeochemical model to the Kattegat-Skagerrak border is underway.

### **Acknowledgement**

This work was funded by the Baltic Sea 2020 foundation. The RCO-SCOBI model simulations were partly performed on the climate computing resource 'Tornado' operated by the National Supercomputer Centre at Linköping University. Tornado is funded by a grant from the Knut and Alice Wallenberg foundation. The models were forced with data from SMHI and Baltic Environmental Database (BED) at Stockholm University.

## References

- Areskoug, H. 1993. Nedfall av kväve och fosfor till Sverige, Östersjön och Västerhavet. Naturvårdsverket, Rapport 4148.
- Eilola, K. and Meier, H.E.M., 2006. Implementation of a high-resolution 3D ecosystem model for local and regional climate studies in the Baltic Sea. Baltex Newsletter, GKSS, Geesthacht, Germany, 9: 10-11.
- Eilola, K., Meier, H.E.M. and Almroth, E., 2008. Modeling phosphorus biogeochemistry in the Baltic Sea. Submitted manuscript.
- Gustafsson, B.G., 2000. Time-dependent modeling of the Baltic entrance area. 1. Quantification of circulation and residence times in the Kattegat and the straits of the Baltic sill. *Estuaries*, 23: 231-252.
- Gustafsson, B.G., 2003. A time-dependent coupled-basin model of the Baltic Sea. C, 47. Earth Sciences Center, Göteborg University, Göteborg.
- Gustafsson, B.G., 2004. Sensitivity of Baltic Sea salinity to large perturbations in climate. *Climate Research*, 27: 237-251.
- HELCOM, 1993, The Second Baltic Sea Pollution Load Compilation (PLC-2), Balt. Sea Environ. Proc. No. 45
- HELCOM, 1998, The Third Baltic Sea Pollution Load Compilation (PLC-3), Balt. Sea Environ. Proc. No. 70
- HELCOM, 2004, The Fourth Baltic Sea Pollution Load Compilation (PLC-4), Balt. Sea Environ. Proc. No. 93.
- Kauker, F., and H.E.M Meier, 2003, Modeling decadal variability of the Baltic Sea: 1. Reconstructing atmospheric surface data for the period 1902-1998, *J. Geophys. Res.*, 108(C8), 3267.
- Kiirikki, M., J. Lehtoranta, A. Inkala, H. Pitkänen, S. Hietanen, P. Hall, A. Tengberg, J. Koponen and J. Sarkkula, 2006, A simple sediment process description suitable for 3D-ecosystem modelling — Development and testing in the Gulf of Finland. *J. Mar. Syst.* 61: 55-66.
- Marmefelt, E. et al., 1999. An integrated biochemical model system for the Baltic Sea. *Hydrobiologia*, 393: 45-56.
- Meier, H.E.M, 2007, Modeling the pathways and ages of inflowing salt- and freshwater in the Baltic Sea, *Estuarine Coastal and Shelf Science*, 74, pp. 610-627.
- Meier, H.E.M. et al., 2003. A multiprocessor coupled ice-ocean model for the Baltic Sea: Application to salt inflow. *J. Geophys. Res.*, 108: doi:10.1029/2000JC000521.
- Meier, H.E.M. and Kauker, F., 2003. Modeling decadal variability of the Baltic Sea: 2. Role of freshwater inflow and large-scale atmospheric circulation for salinity. *J. Geophys. Res.*, C108: doi:10.1029/2003JC001799.
- Omstedt, A. and Hansson, D., 2006. The Baltic Sea ocean climate system memory and response to changes in the water and heat balance components. *Cont. Shelf Res.*, 26: 236-251.
- Savchuk, O.P., 2002. Nutrient biogeochemical cycles in the Gulf of Riga: scaling up field studies with a mathematical model. *J. Mar. Syst.*, 32: 253-280.
- Savchuk, O., Wulff, F., 1996. Biogeochemical transformations of nitrogen and phosphorus in the marine environment - coupling hydrodynamic and biogeochemical processes in models for the Baltic Proper. *Contrib. Systems Ecol.*, Stockholm Univ., 2, 79 pp.
- Savchuk, O., Wulff, F., 2001. A model of the biogeochemical cycles of nitrogen and phosphorus in the Baltic. In: F. Wulff, L. Rahm, P. Larsson (Eds.), *A Systems Analysis of the Baltic Sea*. Springer-Verlag, Berlin, Heidelberg, pp. 373-415.

- Stephanauskas, R., Jorgensen, N.O.G., Eigard, O.R., Zvikas, A., and L. Leonardson, 2002, Summer inputs of riverine nutrients to the Baltic Sea: Bioavailability and eutrophication relevance, *Ecological monographs* 72 (4), 579-597.
- Stigebrandt, A. and Gustafsson, B.G., 2003. Response of the Baltic Sea to Climate Change - Theory and observations. *J. Sea Res.*, 49: 243-256.
- Stigebrandt, A. and Gustafsson, B.G., 2007. Improvement of Baltic proper water quality using large-scale ecological engineering. *Ambio*, 36: 280-286.
- Stålnacke, P., A. Grimvall, K. Sundblad and A. Tonderski, 1999, Estimation of riverine loads of nitrogen and phosphorus to the Baltic Sea, 1970-1993, Wulff, F., A. Stigebrandt, A time-dependent budget model for nutrients in the Baltic Sea, *Global Biogeochem. Cycles*, Vol.3, No1, 63-78, 1989.
- Turner, J.S., 1973. Buoyancy effects in fluids. Cambridge University Press, Cambridge, 368 pp.